

**Design of a Functional Composite Membrane via
Particle Stabilized Emulsion Templating**

by

Selin Kanyas

**A Thesis Submitted to the
Graduate School of Engineering
in Partial Fulfillment of the Requirements for
the Degree of**

**Master of Science
in
Materials Science and Engineering**

Koc University

July 2012

Koc University

Graduate School of Sciences and Engineering

This is to certify that I have examined this copy of a master's thesis by

Selin Kanyas

and have found that it is complete and satisfactory in all respects,
and that any and all revisions required by the final
examining committee have been made.

Committee Members:

Seda Kızılel, Ph. D. (Advisor)

A. Levent Demirel, Ph. D.

Can Erkey, Ph. D.

Date: **10.08.2012**

ABSTRACT

Encapsulation of functional agents within micro-capsules is an attractive technique for controlled delivery where the delivered material is either valuable or corrosive. Emulsion templates are well known to be used for this purpose where the dispersed spherical droplets include functional capsules upon being loaded with functional agents. The challenge of stabilizing immiscible droplets in continuous medium was addressed by particle-stabilized emulsion system, widely known as Pickering emulsions. Partial wetting of the solid particles by the two immiscible liquids leads to self assembly of particles at the liquid-liquid interface during emulsification, providing more stable water-in-oil emulsions compared to the emulsions prepared by known surfactants. The resultant colloid system demonstrated enhanced mechanical strength and viscoelastic behavior. The technique introduced here involves incorporation of micron-sized aqueous phase consisting of functional anti-icing agents into hydrophobic SBS (Styrene-Butadiene-Styrene) copolymer medium and stabilization of the mixture with slightly hydrophobic nanoparticles using emulsion templating method. Partially hydrophobic silica nanoparticles are used to form Pickering emulsion. Gelation of the aqueous dispersed phase is further investigated for additional stability and enhanced control for the release of the anti-icing agent. Aqueous agarose solution is used as a representative gel structure, and the stable emulsion is casted as a membrane upon drying. The membrane is characterized with respect to microstructure and surface water contact angle (WCA). Rheological studies demonstrated that nanoparticle shells around functional beads enhance mechanical strength. The hydrophobicity and thermoplastic nature of SBS polymer allows for incorporation of the composite into other mediums such as bitumen, thus opens possibility to functional delivery of anti-icing agents through mediums which would otherwise not be compatible with polar agents

ÖZET

Fonksiyonel malzemeleri mikro-kapsülleme tekniđi, deđerli veya aşındırıcı malzemelerin kontrollü dağıtımını için ilgi çekici bir tekniktir. Emülsiyon bünyesindeki iç fazda dağılmış damlacıkların malzeme taşıyan fonksiyonel kapsüllere dönüştürüldüğü emülsiyon kalıplama tekniđi yaygın olarak bilinmektedir. Damlacıkları içine karışmadıkları kesintisiz fazla dengeleme zorluğu katı parçacık ile stabilizasyon yöntemi ile aşılabilir. Bu yöntemin Pickering emülsiyonu olarak da adı anılmaktadır. Parçacıkların iki faz tarafından kısmi ıslatılması, damlacık çevresindeki sıvı-sıvı ara-yüzeyde öztoplanma gerçekleştirmesine yol açar. Ortaya çıkan kolloid sistem kontrollü geçirgenlik, mekanik kuvvet ve viskoelastik özellik sağlar. Bu çalışmada, parçacık stabilizasyonu ve emülsiyon kalıplaması kullanılarak, su içeren mikron büyüklükteki damlacıklar buz çözücü malzemeyle yüklenip hidrofobik SBS (Stiren-sütadiyen-stiren) kopolimer ortamına gömülmüştür. Kısmi hidrofobik silika nano-parçacıklardan faydalanılmıştır. Su içeren iç fazın jelleştirilmesinin stabiliteye ve buz çözücü malzemenin kontrollü salımına etkisi incelenmiştir. Temsili bir jel olarak agaroz jel kullanılmıştır. Stabilize edilmiş emülsiyon bir zar oluşturacak şekilde kurutularak kalıplanmıştır. SBS kompozit zar mikro-yapı ve yüzeydeki suyun kontak açısı özellikleri bakımından karakterize edilmiştir. Reolojik çalışmalar fonksiyonel parçacık kafeslerinin ve parçacık miktarının mekanik özellikleri kuvvetlendirdiđini göstermiştir. SBS polimerinin hidrofobik ve termoplastik yapısı geliştirilen kompozit malzemenin bitüm gibi diđer apolar ortamlara entegre edilebileceđini gösterir niteliktedir. Bu sayede buz çözücü polar malzemelerin normal şartlarda uyumlu olmadığı ortamlara katımı ve fonksiyonel salımı gerçekleştirilebilir.

ACKNOWLEDGEMENTS

I would like to offer my respectful gratitude to Assist. Prof. Dr. Seda Kızılel for her advices, discipline and supervision. Her academic approach was truly valuable to me and her sympathetic guidance has encouraged me to be devoted to my research.

I would like to thank Dr. Rıza Kızılel for his support and useful comments about this study. His willingness to help, his kindness and good company and experience were most contributive to shape my academic self.

I would like to thank gratefully to my committee member Prof. Dr. A. Levent Demirel for the attention, time and suggestions through which he contributed to this study. He has kindly offered me access to essential equipment in his laboratory such as the optical microscope and contact angle measuring device.

I would like to thank Prof. Dr. Can Erkey for honoring me by being my committee member. I believe the confidence and good humor he has shown will guide me to be fruitful throughout my career.

I stand grateful to Assist. Prof. Dr. Özgür Birer for his valuable time and attentive approach to help me improve my research. I am thankful for his will to guide me through surface characterization tools in KUYTAM. I offer heartedly thanks to his graduate students Cansu Yıldırım and Kerem Karakuş for kindly accepting me to their laboratory and guiding me to use the ultra-sonication tip tool. I also benefited from the particular knowledge and skills Ali Bateni has offered me regarding DTA tools. Special thanks to Dr. Barış Yağcı for his guidance through DLS and SEM in KUYTAM.

In addition, it is a pleasure to pay tribute to my dear laboratory colleagues Caner Nazlı, Tuğba Bal, Burcu Kepsutlu and Selimcan Azizođlu for they were the ones to tie me to my aim with their companion, sympathy and sense of humor in the course of difficulties. I would like to thank them for enhancing my mind towards many other essentials in life.

Finally, I would like to acknowledge TÜPRAŞ Company for funding this research and granting the equipment such as optical microscope and the rheometer which are utilized for the course of this research. Special thanks to my colleague and dear friend Ramazan Ođuz Canıaz for joining me in abolishing boundaries between industry and academia.

TABLE OF CONTENTS

List of Tables	_____	ix
List of Figures	_____	x
Nomenclature	_____	xiii
Abbreviations	_____	xiv
Chapter 1: Introduction	_____	1
Chapter 2: Literature Review	_____	4
2.1. Emulsion Templating Method		
2.1.1. Macroporous Monolith Synthesis		
2.1.2. Internal Phase Capsules		
2.1.3. Anti-icing Materials in Emulsion Templates		
2.2. Stabilization Mechanism: Pickering Emulsions		
2.2.1. Gravity Induced Instability		
2.2.2. Droplet Bridging		
2.2.3. Rheological Aftermaths of Particle Stabilization		
2.2.4. Gelling of the Internal Cores		
2.3. The Functional Membrane via Particle Stabilized Emulsion Templating		
2.3.1. Justification of the Material Choices		
Chapter 3: Experimental Section	_____	21
3.1. Materials		
3.2. Methods		
3.2.1. SBS Polymer Characterization		
3.2.2. Preparation of the emulsion template		

3.2.2.1. Preparation of the emulsion with Agar domains		
3.2.2.2. Preparation of the emulsion without Agar domains		
3.2.3. Casting the emulsions		
3.2.4. Optical Microscope Observation		
3.2.5. Water Contact Angle Measurements		
3.2.6. Rheological Characterization		
Chapter 4: Results and Discussion	_____	27
4.1. Overview		
4.2. Characterization of SBS		
4.3. Comprehensive Study of Various Emulsion Stabilization Methods		
4.4. Solid Particle Stabilization and Gravity Induces Instabilities		
4.5. Casting Emulsion Templated Membranes		
4.5.1. Morphological Studies		
4.5.1.1. Gelling effect		
4.5.1.2. Particle Concentration Effect		
4.5.1.3. Internal Volume Fraction Effect		
4.5.2. Average Wet Droplet/Dry Domain Size Investigation		
4.5.3. Surface Characterization		
4.5.3.1. Relating Morphological Characteristics to Surface Behavior		
4.5.4. Rheological Characterization		
Chapter 5: Conclusion	_____	77
Bibliography	_____	80
Vita	_____	87

LIST OF TABLES

Table 3.1 The list of the parameters changed for investigation of their effects on emulsion templates

Table 4.1. Average droplet/domain sizes (μm) for all samples in wet and dry states with respect to internal volume fraction (horizontal) and particle concentration % (vertical)

LIST OF FIGURES

Figure 2.1 Statistics for traffic accidents on out of ordinary conditioned road ways in 2010 in Turkey, according to the Turkish Statistics Board documentation.

Figure 2.2. Schematic representation of particle stabilized emulsion.

Figure 2.3. Schema of the designed functional composite coating. Arrows represent the proposed release of anti-icing agents.

Figure 2.4. Comparison of the freezing point depression effects of various ionic salts. The bars are to the scale with respect to each other.

Figure 4.1 Dynamic Thermal Analysis (DTA) for SBS

Figure 4.2 Differential Thermal Gravimetry (DTG) for SBS.

Figure 4.3 Emulsion of KCOOH (aq) within SBS polymer solution, without stabilizing agent a) wet state and b) dry state

Figure 4.4 Emulsion of KCOOH (aq) within SBS polymer solution, with SDS surfactant as the stabilizing agent a) wet state and b) dry state

Figure 4.5 Emulsion of KCOOH (aq) within SBS polymer solution, with PMS as the stabilizing agent a) wet state and b) dry state

Figure 4.6 The appearances of mixtures of same components, prepared under different conditions a) Without any additional stabilizer agent b) Particle stabilized homogeneous emulsion

Figure 4.8 Gravity induced sediment phase of an emulsion stabilized by nanoparticles.

Figure 4.7 Demonstration of gravity induced instabilities in nanoparticle stabilized emulsions. a) 0.17 internal volume fraction and 0.7 % wt nanoparticle concentration b) 0.33 % internal volume fraction and 0.7 % wt nanoparticle concentration. Left couple: Immediately after emulsification. Right couple: After gravity induced sedimentation.

Figure 4.9 Micrographs of the wet emulsion with 3 % internal volume fraction and 0.7 % wt nanoparticle concentration. a) Droplets without agar gel. b) Gelled droplets. Scale bar is 200 μm .

Figure 4.10 Micrographs of the templated membranes after drying of the wet casts displayed in Figure xyz. a) Domains without agar gel. b) Gelled domains. Scale bar is 200 μm .

Figure 4.11 Micrographs of wet emulsions with gel droplets, 0.1 internal volume fraction and particle concentration of a) 0.4 % b) 0.7 % c) 1.0 %

Figure 4.12 Micrographs of emulsion templated dry membranes consisting gel cores, 0.10 internal volume fraction and a) 0.4 % wt. particles b) 0.7 % wt. particles c) 1.0 % wt. particles.

Figure 4.13 Micrographs of wet emulsions with gel droplets, 0.7 wt. % particles and internal volume fraction of a) 0.10 b) 0.17 c) 0.33

Figure 4.14 Micrographs of emulsion templated dry gel domains with 0.7 wt. % particles and internal volume fraction of a) 0.10 b) 0.17 c) 0.33

Figure 4.15 Average droplet sizes with respect to nanoparticle concentration for various internal phase fractions in wet emulsion state (without gel).

Figure 4.16 Average domain sizes with respect to nanoparticle concentration for various internal phase fractions in dry membrane state (without gel).

Figure 4.17 Average droplet sizes with respect to nanoparticle concentration for various internal phase fractions in wet emulsion state (with gel).

Figure 4.18 Average domain sizes with respect to nanoparticle concentration for various internal phase fractions in dry membrane state (with gel).

Figure 4.19 Matrix of optical microscope images for wet emulsions without gel cores under magnification

Figure 4.27 Droplet size distribution by fraction for 0.17 int. vol. fraction and 1.0 % wt. particles a) gelled droplets (Average size = 120.65 μm) b) free of gel (Average size = 74.89 μm)

Figure 4.28 Droplet size distribution by fraction for 0.33 int. vol. fraction and 1.0 % wt. particles a) gelled droplets (Average size = 74.3 μm) b) free of gel (Average size = 55.13 μm)

Figure 3.29 WCA ($^{\circ}$) measurements for emulsion templated functional membrane of different compositions without gel. Each series represents an internal volume fraction as displayed in the legend. Horizontal axis represents particle concentration in wt. %.

Figure 3.30 WCA ($^{\circ}$) measurements for emulsion templated functional membrane of different compositions with gel. Each series represents an internal volume fraction as displayed in the legend. Horizontal axis represents particle concentration in wt. %.

a) Immediately after deposition of water droplets on the surface. b) 15 seconds after water droplet deposition on the surface.

Figure 3.31 WCA ($^{\circ}$) measurements for only SBS coating, 1% wt/vol Agar gel with 0.5 g/ml KCOOH (aq) and 1.5% wt/vol Agar gel with 0.5 g/ml KCOOH (aq) a) Immediately after deposition of water droplets on the surface. b) 15 seconds after water droplet deposition on the surface.

Figure 3.32 Dynamic WCA and its change in time (seconds) for the samples which demonstrate water absorption behavior. All emulsion samples are prepared with 1% Agar gel.

Figure 3.33 5 μ l water droplet on the membrane which was templated from the emulsion of internal volume fraction 0.33, and particle concentration 0.7 % a) immediately after disposal of droplet (WCA = 80°) b) 1.5 seconds after (WCA = 25°) c) 2 seconds after disposal of drop (WCA = 13°)

Figure 3.34 Viscosity vs. shear rate plot for four gelled emulsions and homogeneous SBS solution.

Figure 4.35 Viscosity vs. shear rate plot for four gelled emulsions and homogeneous SBS solution.

Figure 4.36 Loss and storage moduli in response to frequency for the template emulsion of gel cores, 0.7 % wt. particle concentration and 0.17 internal phase fraction.

Figure 4.37 Loss and storage moduli in response to frequency for the template emulsion of non-gel cores, 0.7 % wt. particle concentration and 0.17 internal phase fraction.

NOMENCLATURE

ΔE	Energy change upon attachment of a particle on the interface
$\gamma_{O/W} \gamma_{P/W} \gamma_{P/O}$	Interfacial energies of oil-water, particle-water, particle-oil interfaces
k_{BT}	Boltzmann constant
ΔT_F	Decrease in the freezing temperature ($^{\circ}C$)
K_F	Cryoscopic constant
b	Molality of the salt solution (mol/kg)
i	Van't Hoff factor
θ	Interfacial contact angle
o/w	Oil-in-water emulsion
w/o	Water-in-oil emulsion
ϕ	Internal volume fraction
η	Viscosity (Pa.s)
G'	Storage modulus
G''	Loss modulus

ABBREVIATIONS

<i>SBS</i>	Styrene-Butadiene-Styrene block copolymer
<i>HLB</i>	Hydrophilic-lipophilic balance
<i>HIPE</i>	High internal phase emulsion
<i>SDS</i>	Sodium dodecyl sulfate
<i>PANI</i>	Polyaniline
<i>PMS</i>	Potassium methyl siliconate
<i>PMB</i>	Polymer modified bitumen
<i>LVR</i>	Linear viscoelastic region
<i>WCA</i>	Water contact angle (°)

Chapter 1

INTRODUCTION

Incorporating functional materials into immiscible mediums in non-viscous or elastic structures has been a conventional challenge in materials science. This challenge can be met by formation of stable liquid emulsions and using them as templates to form solid-like composites. Emulsion templating is a technique which makes use of the stability of emulsion droplets. [1-11] This method requires drying of the emulsion without deforming the interfacial borders between the dispersed and the continuous phases. It yields structures whose microstructure and morphology depend greatly on the parent emulsion. Two main approaches are well established. In one approach, the continuous phase is mechanically set by polymerization and crosslinking. Subsequently the internal droplet phase which comprises a volatile liquid is being evaporated. The resultant structure is a cross-linked polymer which consists macro-pores due to the voids that the internal phase liquid leaves behind. Such macroporous polymers are applicable for wide purposes such as catalytic storages, filtering systems, optical band-gaps. [2, 3, 6, 7, 12, 13] In the second approach, the stable droplets are covered either by a shell of layer of particles or by a cross-linked polymer monolayer. The continuous phase which is a selected volatile liquid is forfeited to isolate

individual micro-capsules. [1, 4, 10, 11] Such capsules are suggested as encapsulation and delivery systems for functional materials, tools for food processing or cosmetics.

This study involves detailed characterization of templating emulsions which leads to formation of solid-like composites as a result of merging of two well-established approaches. Thus, here, functional material loaded capsules are embedded into a polymeric medium and the resultant elastic material is cast as a membrane.

The functionality of the internal medium is achieved by incorporation of potassium formate salt (KCOOH) which shows strong anti-icing behavior on surfaces. All ionic salts have anti-icing property on surfaces when dissolved in water, since the freezing point depression occurs when the interactions between water molecules are disturbed by foreign atoms in the medium. KCOOH is particularly effective in depressing freezing point of water due to its extremely high water-solubility and water affinity. [14, 15]

By designing a hydrophobic polymeric membrane which consists KCOOH anti-icing agent loaded packages, a moderately hydrophobic anti icing surface coat is obtained, where the challenge of incorporating water-soluble anti-icing materials into a hydrophobic medium is addressed. The distribution of functional packages on the surface is highly dependent on the distribution of internal phase droplets in the parent emulsion prior to drying. Particle stabilization method is employed for the long-term stability of the emulsion template. Particle stabilization method for emulsions is an advantageous alternative to conventional surfactant molecules. Micro or nano-sized particles are adsorbed at the interface of two immiscible liquid when the interfacial energy between the liquids is high enough and when the particle surface is partially wettable by both surfaces. The emulsions prepared by this method is known as “Pickering emulsions” which was originally described as the phenomenon of particle coverage of emulsion droplets. [16-19] Apart from stabilization, particle shells also play role in controlled permeability. Adjusting the size of the particles determines the voids between them and consequently the area from which encapsulated

functional material can be released. Such controlled release possesses great importance in the use of anti-icing materials since these water soluble materials tend to be carried away with water and get wasted before their function is served. Furthermore, excess amount of anti-icing material release has corrosive consequences.[14, 15]

The polymer that constitutes the continuous phase of the parent emulsion and the membrane base of the resultant composite is styrene-butadiene-styrene (SBS) block copolymer. SBS is widely used in polymer modified bitumens (PMB) for the construction of asphalt binders. [20-30] The compatibility of SBS in bituminous mediums opens possibility to incorporate this system into applications where bitumen can be rendered anti-icing functional as a result of effective incorporation of functional packages.

The functional packages incorporated into the polymer medium is further designed to promote gelation, so that mechanical and rheological properties can be promoted. The presence of the gel phase not only reinforces the mechanical strength, but also contributes to the enhanced stability of the parent emulsion.

This study integrates phenomena on interfacial energies (particle stabilization), intermolecular interactions (anti-icing agents), rheology (gelling and elasticity) while merging two well known emulsion templating approaches. The additional novelty introduced here involves loading of anti-icing agents into micron-sized packages, which will be useful to reduce ice formation on surfaces for various applications.

Chapter 2

LITERATURE REVIEW

2.1. Emulsion Templating Method

Emulsion template is a method where solid structures and scaffolds are produced by using stable emulsion droplets as templates around which solid material is grown. [1-13, 31-34] This technique has described as a tool for the two main approaches introduced by various authors and described in the following sections.

2.1.1. Macroporous Monolith Synthesis

The first of these approaches yields to porous monolith materials. [2, 3, 6, 7] This approach requires transformation of the continuous phase of an emulsion into a solid matrix. Subsequently, dispersed droplets are forfeited by evaporating or dissolving in a suitable liquid, leaving spherical pores behind. [6, 7] Such porous monoliths are attractive potential materials for filtering aerosols. Imhof and Pine [6] have templated micro-emulsions of droplet size ranging from 100 to 200 nm. They have obtained a porous monolith by removal of oil droplets within aqueous continuous medium and gelation of the aqueous medium by sol-gel method.. Sol-gel method is fixing an emulsion structure by galation of the inorganic

medium in which immiscible droplets are dispersed. When the continuous phase comprises an organic liquid, the structure is captured by polymerization. [7]

In a previous study, Binks prepared a porous silica monolith by silica particles alone. [3].

Imhof and Pine have employed sol-gel processing to cure the continuous phase. [6]

Such porous monoliths are also proposed to be used as adsorbents, catalytic supports, lightweight structural materials, insulators besides their potential application as filters. [3, 6, 7, 33]

2.1.2. Internal Phase Capsules

The second approach used as emulsion template method involves precipitation or coating of a target material around the droplets in order to form core-shell structure. [1, 4, 10] The resultant capsules are subsequently isolated from the continuous phase and dried. Wei and Wan pointed out the importance of self-assembly of target materials on the interface to form stable capsules. [10] The authors obtained polyaniline coated hollow microspheres by self-assembly of anilin monomers around oil in water (o/w) droplets in emulsion, and polymerized the shell subsequently.. Such capsules are promising to be used as delivery vehicles for controlled-release encapsulation, drug delivery, protection of biologically active agents. [4, 10]

In general, these two approaches of emulsion templating method have been considered for different applications. Macroporous systems are proposed to serve mostly as filtering systems, whereas the capsules are predicted to encapsulate either nanoparticles [35] or biomaterials such as drugs, food and cosmetics.[1, 4, 10, 11]

2.1.3. Anti-icing Materials in Emulsion Templates

This study has employed particle stabilization, and combined two different emulsion template methods (Macroporous systems and capsule formation) so that controlled release of

the anti-icing agent could be achieved from the functional membrane. The goal here is to merge these two approaches for the design of a functional membrane where anti-icing agent is loaded within the embedded capsules..

Anti-icing functionality has urgent need in industry. For example, among many exceptional road conditions, icy roads lead to the largest number of accidents, which is demonstrated in Figure 2.1, based on the traffic accident statistics of 2010 for Turkey.

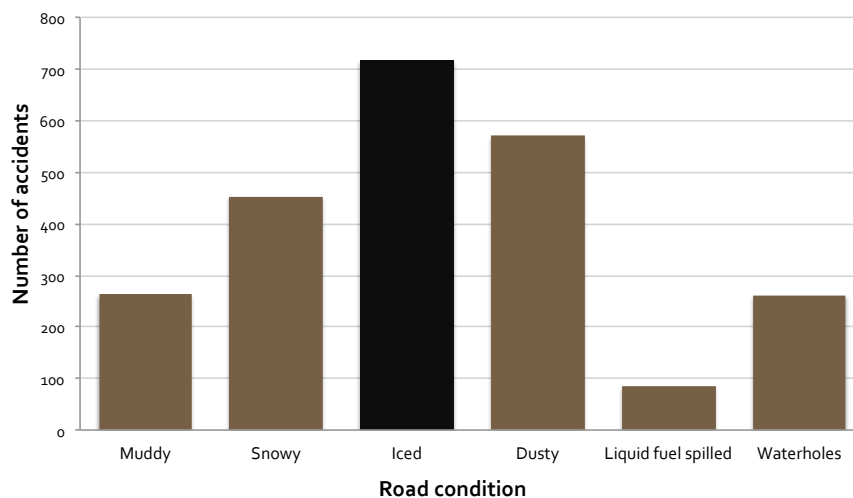


Figure 2.1 Statistics for traffic accidents on out of ordinary conditioned road ways in 2010 in Turkey, according to the Turkish Statistics Board documentation.

Until recently, studies on anti-icing surfaces are predominantly associated with the goal of achieving super-hydrophobicity on surfaces. [36-42] However, superhydrophobicity is not necessarily appealing on all surfaces that require anti-icing functionality. Upon exposure to water, superhydrophobic surfaces promote slip since they reduce drag by trapping gas bubbles between the surface and the liquid in a microscopic texture. [36, 40] Hence, if the reason to avoid icy layer is to hinder slipperiness, superhydrophobic behavior would harm the purpose. Furthermore, surface geometry modification at nano-level is demanding and in most cases economically not feasible.

Another approach to eliminate ice formation on surfaces is the use of anti-icing agents. Ionic salts are the most commonly employed agents for this purpose. As ions are dissolved in water, ionic molecules which localize between water molecules retard the crystallization process. Therefore, water remains in liquid phase at lower temperatures than its normal freezing point. However, the anti-icing materials which are the most effective are expensive, and are wasted as these materials are washed away by the water in which they are dissolved. Furthermore, such water-soluble materials are polar and are not compatible with non-polar surfaces. Hence, use of anti-icing agents are not applicable in hydrophobic mediums. Here, we design a composite membrane coat, which integrates a hydrophobic adhesive base and hydrophilic aqueous phase that incorporates anti-icing agent.

Previously, Dubois et al. developed new techniques to incorporate hydrophilic anti-icing materials into hydrophobic mediums. One of the techniques the author suggested requires encapsulation of ionic salts within cross-linked shells of linseed oil. This shell is of such material that it is elastic at high temperatures whereas brittle at low temperatures. The study is promising as it may be possible to incorporate anti-icing material loaded capsules in hydrophobic mediums such as bitumen. The deviance of brittleness with respect to temperature yields a temperature dependent functionality of the material developed. At high temperatures, where no ice formation occurs, the functional material is protected within the elastic shells. At low temperatures, the shell capsules crack upon pressure and releases the anti-icing material towards the surrounding environment. [43] The second approach developed by the same authors includes incorporation of ionic anti-icing materials within styrene-butadiene-styrene (SBS) polymer medium by the stabilization of a compact amphiphilic molecule, namely potassium methyl silicate (PMS), which is also known to be effectively used in fabrication of water-proof materials. [44]. It is suggested to cast the polymeric slurry as a membrane on a surface to promote controlled release of anti-icing materials, [32] however the details related to the formation of a stable emulsion is not

provided.

Similar to the approach suggested by Dubois et al., the functional membrane designed in this study consists of a base which is the non-polar SBS block copolymer, which can be compatible with most non-polar surfaces. The hydrophilic domains include spherical droplets that store and induce controlled release of the anti-icing agent, selected as potassium formate salt (KCOOH) ions due to its desirable properties. These two immiscible phases, which embody contradictory chemical characteristics, are initially prepared within a stable emulsion. The hydrophilic liquid droplets are dispersed in a polymer solution medium in the emulsion. Emulsion template method involves formation of the elastic membrane platform based on the continuous polymer phase; while the functional domains, which are templated from the dispersed droplets of the initial emulsion, are spread on the solid platform at a macroscopically homogeneous order. Emulsion stabilization prior to drying offers the possibility to integrate two opposite surface properties in a resultant elastic membrane. Previously employed emulsion template studies involved the removal of either dispersed or the continuous phase of the parent emulsion, where no functional agents were introduced into any of the emulsion phases. Through the design presented in this study, the existing emulsion template studies were combined, where the dispersed phase or the continuous phase of the parent emulsion was not sacrificed, and functionally loaded aqueous droplets formed a stable emulsion within the hydrophobic continuous phase with the aid of surface functional nanoparticles. .

The use of emulsions to template solid composite materials provides the advantage of producing three-dimensional structural materials without complications of micromachining. The choice of materials and environmental conditions during templating however, requires more tedious handling. Two main requirements have to be considered. [7] The continuous and dispersed liquids have to be mutually insoluble; and form firmly stable droplets within continuous medium have to be formed.

2.2. Stabilization Mechanism: Pickering Emulsions

Emulsion template method additionally requires a robust and long-term stability of the emulsion droplets to maintain the structure throughout the drying process. [7] Although micro-emulsions, whose droplets are in the order of nanometers, are thermodynamically stable and requires little attention for a stabilizing system [6], emulsion droplets tend to coalesce and phase separate before the templating process, unless caution is taken. [7] It is well established that, as an alternative to surface active molecules, small solid particles attach at fluid/fluid interfaces of two immiscible mediums when the particles are partially wettable by both mediums. [17, 45, 46] This mechanism was pioneered to stabilize emulsions nearly a century ago. [19, 47] Attributing to one of the lead scientists who introduces solid particle stabilized emulsions, such emulsions are also known as “Pickering emulsions”. Recently, Pickering emulsions have become preferred approach for the use in emulsion templates due to their strong stability.

Attachment of Pickering particles at the interface is energetically thermodynamically favorable phenomenon. Fixation of a particle at an interface decreases the entropy, which reduces the total free energy. . The interfacial energies of the particle oil interface ($\gamma_{P/O}$), the particle-water interface ($\gamma_{P/W}$), the oil-water interface ($\gamma_{O/W}$) and the effective radius of the particle (R) contribute to the free energy change due to a single particle attachment (Eqn. 1). [3, 48]

$$\Delta E = - \Pi r^2 / \gamma_{O/W} \times [\gamma_{O/W} - \gamma_{P/W} - \gamma_{P/O}]^2 \quad \text{Eqn. 1 [48, 49]}$$

This energy favor is higher than the thermal energy of particles coming together with the kinetic energy of the Brownian motion for Pickering particles. Consequently, the particle adsorption is irreversible[50]. Thus, once a particle is attached, it is not delocalized;

although Russell et al. points out the spontaneous tendency of extremely small particles to be displaced after attachment. [48] The reason that Russell et. al. mentions the possibility of detachment of extremely small particles is because ΔE in Eqn. 1 increases linearly with r^2 and thermal energy is sufficient to detach extremely small particles (~ 16 nm) from the interface. Correspondingly, in Pickering emulsions, adventitiously introduced larger particles displace the smaller ones from the interface to replace them. [48] Nevertheless, Pickering particles consist of a range from nanometer up to micrometer size [51] and their attachment to the interface is principally irreversible. [44, 52].

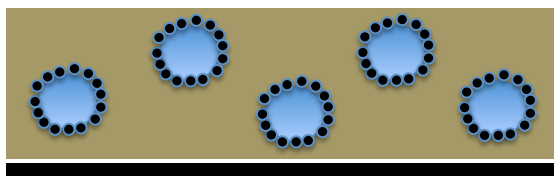


Figure 2.2. Schematic representation of particle stabilized emulsion.

The irreversibility of the attachment is a striking difference and an advantage relative to stabilization with conventional surfactant molecules. The very high energy of attachment of particles to interfaces yields remarkable stability against coalescence which surfactant molecules do not perform. [3] Unlike Pickering particles, surfactant molecules are held at the interface by dynamic equilibrium; they rapidly adsorb and desorb at the interface, which makes their stabilization weaker. [53]

Analogous to a surfactant molecule's hydrophilic-lipophylic-balance (HLB), particle's wettability at the oil water interface determines the adsorption behavior at the interface. [16, 54]

For partially hydrophilic particles, the interfacial contact angle θ measured into the aqueous phase is $<90^\circ$. Two phase mixtures containing such particles tend to form oil-in-water (o/w) emulsions where the majority of the particles' surface reside in the medium they favor.

Similarly, partially hydrophobic particles with $\theta > 90^\circ$ (e.g. surface treated silica)[3] yield to water-in-oil (w/o) emulsions. It is important to note that in Pickering emulsions, whether w/o or o/w, the particles have to be partially wettable by both surfaces. Particles which are strongly hydrophilic ($\theta < 30^\circ$) or strongly hydrophobic ($\theta > 150^\circ$) have been observed to yield unstable mixture where they reside fully in either one of the phases. Strongest stabilization occurs with particles with $\theta = 90^\circ$ with the attachment energy favor reaching 2750 kT. [3]

Besides material characteristics such as the particle size, shape, hydrophobicity, interfacial energy, experimental conditions such as shear energy applied during emulsification and temperature or dispersed phase volume ratio are determinant factors in stabilizing Pickering emulsions. For instance, Wei and Wan suggested that at high temperatures more stable emulsions form, as at low temperatures droplet coalescence is stimulated. . [10] Needlelike Polyaniline (PANI) particles as polymeric stabilizers have been found to be more effective than spherical particles as stabilizers. [55] Noble and colleagues produced stable w/o emulsions with rodlike polymeric particles as stabilizers. [56]

2.2.1. Gravity Induced Instability

The particle shells conserve the droplets in their stable spherical shapes for long periods of time (> 4 years). However, at volume fractions lower than what is required for closed packing of droplets, gravity induced instability is observed. When the dispersed phase is denser than the continuous phase, the droplets' weight combined with the partial attraction between the particles causes flocculation of the droplets at the bottom of the emulsion. Thus the droplets come nearly in contact but do not fuse. The steric hindrance caused by the particles around them inhibits coalescence. Larger droplets are heavier, thus they enhance gravity induced instability. Increasing the volume fraction of the dispersed phase generally reduces gravity induced instabilities; instead of inducing "catastrophic phase inversion" as in surfactant stabilized emulsions. [3] In common surfactants the phase which has higher

volume fraction tends to be the continuous phase. Catastrophic phase inversion is transition between o/w and w/o emulsion types by changing the volume fraction of the dispersed phase. Stable Pickering emulsions can tolerate very high volume fractions of dispersed phase without catastrophic phase inversion.

High internal phase emulsions (HIPE) are accepted to have a minimum dispersed volume ratio of 74 %. [9, 50] Ikem et. al. have obtained HIPEs of the dispersed phase volume reaching 92 % that did not induce catastrophic phase inversion by utilizing oleic acid functionalized silica particles for stabilization. They have accomplished such stable emulsions simply by stirring. [50]

If the continuous phase is polymerizable HIPEs can be used as emulsion template method for fabrication of light-weight structural materials or scaffolds for tissue engineering. Ikem and colleagues have employed emulsion template method on HIPEs by polymerizing the continuous phase to obtain poly-Pickering HIPEs.[50] This method yielded a robust macroporous polymer monolith. In another study, same authors have quantified the gas permeability rate through the pores which were the internal phase droplets prior to drying. [13] It is clear that when used for emulsion templates, Pickering emulsions retain stability of dispersed droplets even at very high volume fractions during drying. Nevertheless, in certain cases larger fraction of the dispersed phase leads to partial coverage of droplets on the interface instead of a dense layer.

2.2.2. Droplet Bridging

Such reduction in coverage either leads to droplet coalescence or “particle bridging”. Particles can form a monolayer between two droplets, bridging their interfaces.[44, 57-59] This “zipping” or “bridging” mechanism can hinder inter-droplet film drainage at particle concentrations lower than enough to cover each droplet separately. This bridging mechanism hinders inter-droplet film rupture and sustains the droplets in a finite distance.[52] Lee et. al. has defined this bridging effect as the phenomenon where particles attached to a droplet

surface simultaneously adsorbs to another droplet surface and a shared particle monolayer is formed. Such droplet bridging imparts enhanced mechanical stability, thus contribute to rheology.

2.2.3. Rheological Aftermaths of Particle Stabilization

Intensified rheological characteristics of the emulsion is another mechanism behind the versatility of Pickering emulsions. Interparticle interactions in the continuous phase play role in the non-Newtonian flow behavior. At high shear, emulsions show shear-thinning behavior due to destruction of particle interactions in the continuous phase. Thus the system becomes easily processable. [51]

Rheological behavior contributes to emulsion stability as well. Lee et al asserts that rheology and stability dominantly affect stability and function. [44] Highly concentrated, partially attractive particles form aggregates which fill the space between droplets in the continuous phase. A 3D network of particles resulting from particle-particle interactions in the continuous medium causes an increase in viscosity.[50] Thieme et. al. notes the mechanical barrier of particles that impedes coalescence also results in higher viscosity. Moreover, the particle network that extends through the coherent phase contributes to the enhanced viscosity which in return reinforces stability. Particles also impart a high degree of elasticity. [60] For Pickering emulsions stabilized by fumed silica, particles in excess of those required to cover the drop interfaces remain in the continuous phase and form a particle network via siloxane bonds. [3] The viscosity increase due to such space filling network mechanism increases viscosity and retards the motion of droplets in the continuous phase, undermining droplet collisions. The stability which particles impart results in the formation of smaller droplets. The decrease in droplet diameter and increase in emulsion viscosity are interactively determinant. Increased droplet contact which results from formation of smaller droplets, enhances viscosity. [50] In addition, increased viscosity increases shear during

emulsification which leads to smaller, consequently more stable droplets. Furthermore, the particle layer hinders coalescence by imparting viscoelasticity to the interface and retarding thinning of the film between the droplets. [51, 61] This viscoelastic interface reinforces applicability of Pickering emulsions for emulsion template method. Imhof and Pine has pointed out that deformability (e.g. elasticity) of the droplets prevent cracking of the dispersed domains during ageing and drying as a necessity of templating. [6] It is also noted the importance of drying of the emulsion without destructing the shape of the supporting structure at interfaces.[7] Although shrinkage of the template droplets are generally observed in during emulsion templating, cracking, pulverization or ripped surfaces should be avoided. Naturally, both organic and inorganic gels shrink by up to 50 % compared to their wet size during removal of the solvent. However, emulsion templates can retain the curvature and shape of the supported domains [7] The difference in behavior of emulsions stabilized by solid particles and molecular surfactants during drying is studied by Nakagawa and Nonomura in 2011. [62] They have compared emulsions stabilized by spherical silicone resin particles and those stabilized by common surfactants. Nakagawa and Nonomura note that particle shells at the interface are rigid and more difficult to destroy relative to interfaces covered with common surfactants.

2.2.4. Gelling of the Internal Cores

One way to reinforce the curvature and to fix the dispersed domains during emulsion templating is through gelation of the droplets. Several authors used particle stabilization method together with gelation of the inner core. Stable Pickering gel droplets were suggested for their potential use in the delivery and controlled encapsulation of molecules. [35, 44, 63]

Thus, emulsion template method which combines particle stabilization and inner gel cores has **attracted considerable attention.???** Cayre and colleagues [4] have prepared

colloidosome capsules [64] by gelation of the aqueous cores. They have compared the mechanical stability of the capsules that were formed with the gel to the case where the aqueous cores did not include any gel. They concluded that the presence of a gel core is vital to sustain the integrity of their microcapsules.

As the particles restrict the gel cores from merging together, the gel phase enhances the adsorption behavior of particles and supply additional stiffness to the particle shell in particle-stabilized emulsions. Although Imhof and Pine [7] stated that the sole function of a surfactant in emulsion templating process is to stabilize the droplets, it is not the case when particle stabilized emulsions are used as delivery capsules. Besides acting as surfactants for the system, the particle shell also acts as a semi-permeable membrane via the pores between the closed packed layer around the droplets. They function for restricted release of functional materials stored within capsules. Several authors investigated the effect of the particle shells on permeability of the obtained capsules. Duan et. al showed that particle size controls the amount of material release from nanoparticle loaded microcapsules. They prepared w/o emulsions where agarose was added to the water droplets, and crosslinking of the agarose occurred at lower temperatures. The authors demonstrated nano-scale selectivity in permeability by doping different sized nanoparticles in the gel cores. Similarly, Wang et al. moderated alginate gel cores within continuous oil medium.[35] Dinsmore et. al. named such particle shell self-assemblies as “colloidosomes”, a name which has become widely used in the literature. [64, 65]

Thus, gelation of the inner core of colloidosomes have been actively studied in particle stabilized capsules which is only one of the emulsion templating approaches mentioned above[4]. However gelation of the inner cores of an emulsion which templates a monolith has not yet been used. The reason of this defer is that most emulsion templated monoliths in the literature are studied to function as filters or optical band-gaps which require the pores to remain as voids. Therefore, the additional novelty introduced in this study involves the

design of a monolith, in which embedded domains act as delivery capsules to store and release anti-icing materials. In order to enhance immobilization of the functional domains, gelation of stabilized capsules in a continuous polymer medium, captured by emulsion templating method, is suggested in the present study. The presence of gel cores enhance the particle attachment on the droplet interface and impart sufficient stiffness against shear and ambient effects. Such stiffness is responsible to protect the functional domains of the membrane from water or air flow on the surface. Crosslinked structure of the gel phase further contribute to the selective permeability within the cores along with the particle shell. Duan et al.[35] prepared water in oil emulsions where agarose was added to the water droplets which crosslink at lower temperatures. The authors demonstrated the nano-scale selectivity in permeability by doping different sized nanoparticles in the gel cores. Similarly, Wang et al. prepared alginate gel cores within continuous oil medium for the purpose of supporting the particle shell and endowing sufficient stiffness to allow separation of the colloidosomes from the oil phase. [10]

2.3. The Functional Membrane via Particle Stabilized Emulsion Templating

Self-assembled particle shells (i.e. colloidosomes) are have been extensively used in recent years to be used as templates in both of the emulsion template approaches (either the continuous phase or the dispersed phase is propitiatory). Binks developed a macroporous material by stabilizing both w/o and o/w emulsions by using solely silica particles. [3] Niu et al. attracted attention to the generation of novel functional materials with hierarchical ordering and their impact on recent materials science endeavors. [49]

The potential of Pickering droplets for selectively permeable shells makes them good candidates to template emulsions whose continuous phase is disregarded to isolate individual semipermeable microcapsules. Furthermore, Matheson has attracted attention to the fact that nanoparticles had wide possibilities of applications in functional coating systems and membranes. [66] Madej and Russell in separate studies demonstrated the formation of breath figures on polymeric membranes via the self assembly behavior of nanoparticles within polymer membranes. [67, 68]

In this study, for the goal of preparation of a functional membrane coating, Pickering emulsion droplets as templates for the functional domains, which encapsulate anti-icing KCOOH, was used. The advantage of this material compared to the existing ones are the restricted permeability and extreme stability during drying process. In order to avoid destructed shapes as described by Nakagawa and Nonomura, to enhance restricted permeability, and to reinforce rheological properties, the material was designed to include functional domains with agarose gel.

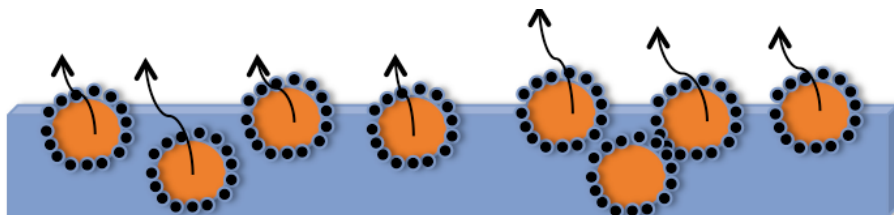


Figure 2.3. Schema of the designed functional composite coating. Arrows represent the proposed release of anti-icing agents.

Initially aqueous agarose solution is dispersed in cyclohexane in the presence of partially hydrophobic silica nanoparticles, followed by incorporation of linear SBS block copolymer dissolved in cyclohexane into the continuous phase. KCOOH salt has been dissolved in the agar solution prior to emulsification. KCOOH was employed as an example of an effective anti-icing agent.

2.3.1. Justification of the Material Choices

Sodium chloride ionic salt (NaCl) is the most commonly used anti-icing agent despite its insufficient function, due to its abundance and low price. Other ionic salts such as Magnesium Chloride (MgCl₂) and Calcium Chloride (CaCl₂) are also used as anti-icers or deicer chemicals. However, such chloride salts have been declared to be toxic by the Canadian Environmental Protection Act. [14] Furthermore, chloride chemicals are environmentally corrosive. Consequently, alternative anti-icing agents have been suggested in various studies. Calcium magnesium acetate, potassium acetate, sodium formate and potassium formate are claimed to be valid candidates to be typically used as anti-icing agents. [14, 69-71] They have attracted attention as a result of their low corrosion and environmentally safe properties. Especially the family of materials which contains potassium have raised interest since there is no drinking water guideline limit for potassium in European Union and Canada. [14] Besides its environmental affinity, KCOOH exceeds most of the ionic chemicals by its anti-icing functionality. The degree of freezing point depression of water when an ionic salt is dissolved is determined by the equation below.

$$\Delta T_F = K_F \cdot b \cdot i \quad \text{Eqn. 2}$$

where ΔT_F is the decrease in the freezing temperature (°C), K_F is the cryoscopic constant which is an intrinsic property of the solute, b is the molality of the salt solution (mol/kg) and i is the van't Hoff factor which is the number of ions per solute molecule. Accordingly, the freezing point depression effect of KCOOH exceeds that of NaCl by multiple times as seen in Figure 2.4.

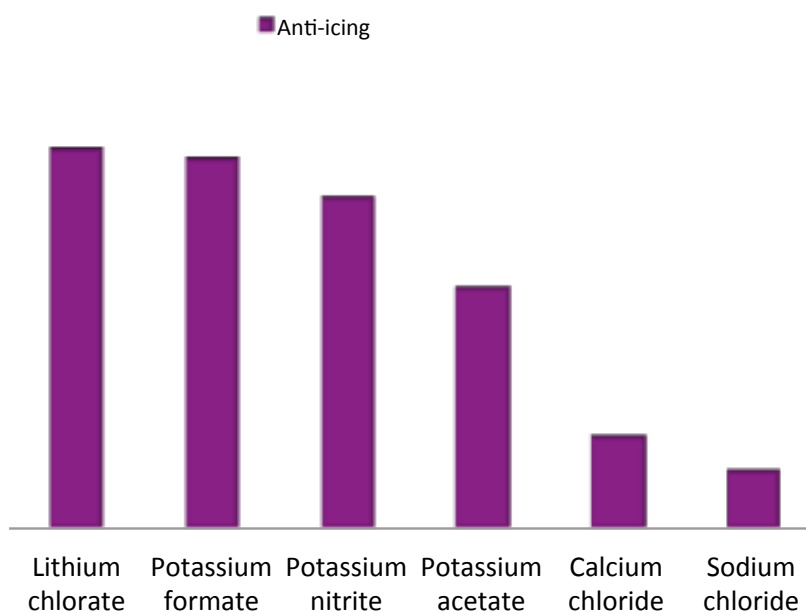


Figure 2.4. Comparison of the freezing point depression effects of various ionic salts. The bars are to the scale with respect to each other.

However, the abundance and economic favor of NaCl offers tolerance for very high amounts of consumption most of which is wasted due to lack of a controlled consumption. For example, in recent years, the annual amount of chloride salts used to hinder icing on roads in Japan, the U.S., Canada and European Countries have reached 50 000 tons. [14] Despite the lacking advantage of NaCl, the use alternative de-icing agents have not made a significant leap yet. This is mainly due to the intolerance for wasting expensive materials.

In the membrane designed here, KCOOH as anti-icing agent have been incorporated, in order to avoid excess salt release through storage within protected domains. Both the particle shell and the gel structure was utilized in order to limit high release of the functional agent.

The choice of the particles to be used for stabilizing parent emulsion and protecting the functional domains is essential, mainly because their chemical characteristic and size determine their absorption behavior as mentioned above. Commercially available AEROSIL® 816 fumed silica nanoparticles as in powder form was used to achieve these goals. On the basis of published values for surface energy of the AEROSIL 816, the nanoparticles are partially hydrophobic. [72, 73]

Simovic et. al. have reported the hydrophobicity index of these silica particles as roughly 0.72 and contact angle as 60°. [72] According to the manufacturer, the particles were produced by surface modification of hydrophilic silica nano-powder with hexadecylsilane. Such silane reagent converts a proportion of silanol (SiOH) groups on the surface to methyl groups, imparting hydrophobicity to the surface.[3] The primary particle diameter is 12 nm. It has a particle density of 2200 kg/m³, SiO₂ content of 99.8% and specific surface area of 190 m²/g. [73]

The hexadecylsilane treated surfaces of the particles tend to interact and agglomerate. Therefore, they require high amount of energy to be de-agglomerated down to nano levels. Ding et al. have reported that after erosion of the bulky agglomerates, the nano-aggregates could not be broken into primary particles even upon exposure to highest energy density. [73]

Following previously done research and studies, this thesis analyses a composite membrane which is templated from an aqueous phase in oil emulsion. The aqueous phase is loaded with functional anti-icing KCOOH salt. The continuous phase constitutes SBS polymer. The template emulsion is stabilized by surface hydrophobized silica nanoparticles via the mechanism of Pickering emulsions. It is aimed to initiate controlled release of KCOOH through the internal phase domains and through the particle shells. The combination of two approaches in emulsion templating and gelation of the stabilized domains offer promising novel methods for functional material loaded surface coating membranes.

Chapter 3

EXPERIMENTAL SECTION

3.1. Materials

Styrene-butadiene-styrene block copolymer (SBS, S:B wt fraction: 70:30) and Potassium formate (KCOOH) salt (99 %) and Sodium dodecyl sulfate (SDS) was purchased from Sigma in powder form. Agarose powder was purchased from Sigma-Aldrich Silica nanoparticles (AEROSIL 816 ®) were kindly supplied by Degussa in powder form. Primary particle diameter of the particles is stated to be 12 nm by the supplier. Cyclohexane (99.9 %), acetone (99 %), ethanol (99 %) were purchased from Merck. Distilled water was obtained through filtering via the distilled water production unit in our laboratory. Glass petri-dishes and glass microscope slides were purchased from Nunc. The stage used to dry and photograph the samples was constructed by Yılmaz Torna in Istanbul.

3.2. Methods

3.2.1. SBS Polymer Characterization

In order to analyze the degradation temperature limit of the SBS polymer used in this study, Dynamic Thermal Analysis (DTA) and Thermal Gravimetric Analysis (TGA) were utilized. DTA/TG (SII EXSTAR 6300) analyses were conducted under the argon gas flow from room temperature to 520 °C at the heating rate of 10 °C/min using Aluminum (Al) sample holders. In each test near to 10 mg sample was loaded in to Al sample holders.

3.2.2. Preparation of the emulsion template

A total of 18 emulsions each constituting a different composition of components were prepared.

Commercially obtained, silica AEROSIL 816 ® nanoparticles with average primary particle diameter of $D = 12$ nm were dispersed in cyclohexane with three different concentrations: 0.4 % wt, 0.7 % wt. and 1.0 % wt. The dispersion was carried out by high energy application via ultra-sonication tip (73 MS, 50 % amplitude, 50 Hz frequency) for 3 minutes. Ice bath was applied every 45 seconds to avoid over rises in temperature. During the period between nanoparticle dispersion and emulsion preparation, the nanoparticle suspension is kept in ultrasonic bath in order to avoid agglomerations due to steady positioning. DLS measurements have indicated that full avoidance of agglomeration has not been achieved. Nanoparticle dispersions of all concentrations outturned particle sizes of the range 100-150 nm.

The SBS stock solution is prepared by mixing 110 mg/ml SBS in cyclohexane. The mixture is stirred on magnetic stirrer at room temperature.

3.2.2.1. Preparation of the emulsion with Agar domains

Agarose solution is prepared by adding 1 % wt Agar powder in distilled water. The mixture is cooked in microwave oven until it boils and all powder is dissolved. Subsequently 0.5 g/ml KCOOH (s) salt is added very slowly. Emulsification is spread over a time period of 8 minutes while the agar solution is kept being stirred at 100 °C on the magnetic stirrer. Three different fractions of internal volume of salty agar solution was added into three different concentrations of nanoparticle-cyclohexane dispersion. The particle dispersion was kept at room temperature. (Nanoparticle concentrations: 0.4 wt %, 0.7 wt %, 1.0 wt. %. Internal volume fractions: 0.10, 0.17, 0.33) The internal aqueous phase is introduced to the continuous polymer solution phase under high shear applied by vortex at maximum

speed for 5 seconds. As the hot agarose solution is dispersed into the cyclohexane, the aqueous solution forms well dispersed droplets which are stabilized by the nanoparticles. The stabilized agarose droplets instantly cool as they meet the medium at room temperature. Agarose solution becomes gel, thus gelled aqueous droplets dispersed in cyclohexane is formed as an emulsion. Subsequently, 1 ml of the concentrated SBS polymer dissolved in cyclohexane (110 mg/ml) was drop-wise added into the continuous phase of the prepared emulsion while gently shaking.

Internal volume fraction is calculated by the ratio of the aqueous phase volume to the total volume of the final emulsion.

3.2.2.2. Preparation of the emulsion without Agar domains

KCOOH salt in solid form is freed from moisture through dry freezing. An aqueous KCOOH stock was prepared by dissolving the salt in distilled water at room temperature. In order to obtain emulsion templates with no gel in the dispersed phase, the procedure explained above is applied with using simple KCOOH solution that does not contain any agarose as the internal phase at room temperature. The stability of the emulsions are observed by leaving the vials containing them untouched for 3 days.

A total of 36 sample emulsions each constituting a different composition of components were examined. The table below shows the values for each parameter that were investigated for the emulsions.

Table 3.1 The list of the parameters changed for investigation of their effects on emulsion templates

Internal Volume Fraction	0.10	0.17	0.33
Nanoparticle Concentration % weight	0.4 %	0.7 %	1.0 %
Droplet composition	Agar Gel	Non-gel	

3.2.3. Casting the emulsions

Glass microscope slides were cut as square substrates with 2 (width) – 2 (length) cm dimensions with the use of a diamond tipped cutting tool in a dust-free environment. They were treated with ethanol and rinsed with distilled water. After the glass substrates are dry, 100 μl of each emulsion is deposited on a glass slide. The wet emulsions on the substrate were spread over an area of 0.75 cm^2 by slightly shifting the glass with circular movements. This way, thinning of the cast emulsion annihilates cracks that are possible to occur during the unequal rate of evaporation of water in aqueous phase and the cyclohexane in the organic continuous phase. The cast membranes on glass slides are left

to dry at 15 °C. When enough amount of solvent evaporated from both phases of the emulsion so that the membranes appeared elastic, they were considered to be dry.

3.2.4. Optical Microscope Observation

Both wet and dry samples were visualized using optical upright microscope (Nikon, Eclipse Ni-U). 5x and 10x objectives were used. Optical micrographs were obtained by placing wet emulsion samples on previously cut square shaped glass slides with the cast side up. They were then placed in an optical microscope attached to a DS camera control unit (Model: DS-L3) either before or after solvent evaporation. The surface image was imported to a software program (Kameram) for analysis of droplet sizes and morphologies.

3.2.5. Water Contact Angle Goniometry

WCA (water contact angle) on surfaces of dry cast membranes were determined on a contact angle system (DataPhysics Instruments, Germany) at room temperature and ambient relative humidity. The membrane surfaces had 0.5 - 1 cm² surface area. The membranes are kept in glass petri dishes which had previously been rinsed with ethanol and deionized water throughout the drying process. They are characterized after enough solvent has evaporated so that they no longer flow, without further processing. A water droplet of 5 µl was deposited on the surface of each dry membrane by micro-syringe and the contact angle it makes with the surface was measured. Three individual membranes for every sample emulsion and three different positions on each membrane were characterized with WCA. The experimental set-up integrates a black and white displayed video camera

mounted with magnifier. The video signal is transmitted to a computer software to import the drop image. The contact angles were obtained by the sessile drop method.

3.2.6. Rheological Characterization

Rheological measurements were performed at 25 °C using a stress-strain controlled rheometer. (Discovery Hybrid Series-2) from Thermal Analysis (TA) Instruments with a profiled parallel-plate geometry (20 mm plate diameter). Experiments were carried out with a mechanically set gap of 950 μm . Flow tests were conducted to determine viscosities of the wet emulsions by gradually increasing shear rate from 0.01 to 100 1/s. Oscillatory tests were conducted to measure G' and G'' (storage and loss moduli) of the wet emulsions by frequency sweep from 1 to 100 Hz with a set strain of 0.2 %. The linear viscoelastic region (LVR) was determined by running a strain sweep test between 0.1 % and 100 %. LVR was detected by the range which viscosity was constant. LVR was between 0.1% and 10% on log scale.

Chapter 4

RESULTS AND DISCUSSION

4.1. Overview

A novel polymeric composite membrane based on an emulsion template with functional dispersed droplets with or without gel phase was synthesized and characterized in detail. The droplets were functionalized by loading with aqueous KCOOH as a representative anti-icing agent. The choice of KCOOH as the functional material was based on its enhanced effectiveness in depressing freezing point of water and its non-corrosive nature compared to other common ionic salts, as was mentioned in the introduction part. Emulsion was stabilized by solid particle stabilization method, utilizing surface modified partially hydrophobic silica nanoparticles. Aqueous KCOOH droplets, despite being incompatible with any hydrophobic medium due to its water soluble characteristics, were embedded into continuous hydrophobic SBS copolymer solution through emulsion stabilization. The stabilized emulsion was subsequently cast on a smooth glass surface to yield a membrane in the form of a hydrophobic surface coating upon evaporation of the solvent from both phases. The resultant structure was functionally loaded hydrophilic beads with nanoparticle shells around them embedded into a solid hydrophobic polymer membrane.

4.2. Characterization of SBS

SBS was chosen as the continuous medium of the emulsion, due to its adhesive, elastic and chemically durable properties. SBS can modify various hydrophobic mediums by integration into those mediums. [20-30] In addition, glass transition temperature, durability against high temperatures, compatibility with various hydrophobic mediums (e.g. bitumen), abrasive resistance and rheology are the main reasons for incorporation of SBS into the novel emulsion system developed here. Rheological characterization of SBS will be presented in the following sections. In order to quantify the stability of SBS against high temperatures, Dynamic Thermal Analysis (DTA) and Thermal Gravimetric (TGA) analysis have also been performed.

DTA is a method to measure heat flow as solid material goes through various changes due to temperature increase. This measurement detects the temperatures at which material gets modified and plots them as changes in heat flow in or out of the system depending on whether the modification is exothermic or endothermic. The method yields accurate results that are indicator of both chemical and physical changes within the material structure.

TGA is a very precise measurement system of weight of a solid material in relation to temperature. Therefore it tracks the temperature where solid phase of the material begins to decompose into gas. Different from from Dynamic Thermal Analysis (DTA), TGA is a solely determinant of chemical decompositions and chemical changes.

SBS copolymer in use has proven to be stable at a temperature as high as 400 °C. Above 400 °C chemical decomposition occurs as was observed by DTA and TGA (Figures 4.1 and 4.2)

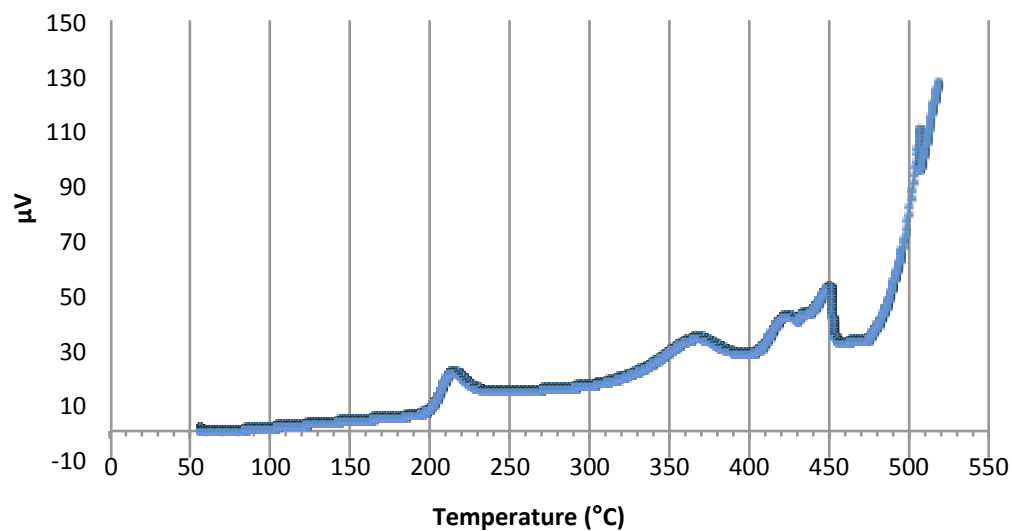


Figure 4.1 Dynamic Thermal Analysis (DTA) for SBS

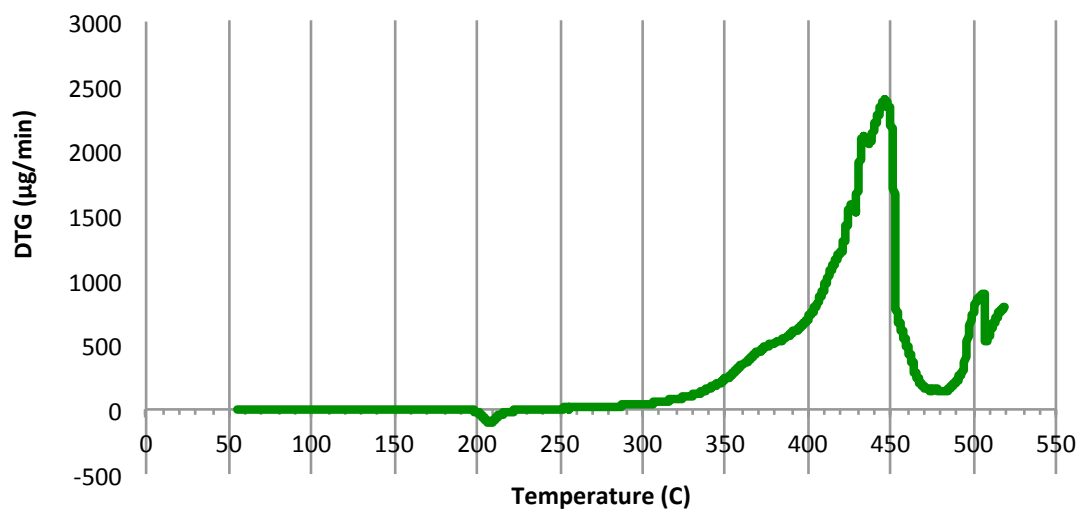


Figure 4.2 Differential Thermal Gravimetry (DTG) for SBS.

Durability of SBS polymer against high temperatures is important, as this allows for the use of this polymer in hydrophobic mediums that require high temperature process conditions for preparation, and contributes to the mechanical stability of the resultant product. For example, the fact that SBS remains intact without degradation at high temperatures opens the possibilities for the use of a designed composite material that include SBS to be incorporated in bitumen at its process conditions.

4.3. Comprehensive Study of Various Emulsion Stabilization Methods

The main objective in this study is to transform a double phase emulsion into a solid membrane which constitutes materials that of both phases homogeneously. The primary requirement for such emulsion templating is to maintain the internal phase droplets in a fairly stable state until after emulsion is dried as a solid membrane.

In order to investigate the stabilization potency of different mechanisms, emulsions prepared via different methods were compared. Emulsions were prepared without any additional stabilization attempt, then they were prepared by a long tailed ionic surfactant sodium dodecyl sulfate (SDS). Next, a small and compact amphiphilic molecule Potassium Methyl Siliconate (PMS) was chosen, and finally surface modified hydrophobic silica nanoparticles (ARO 816®) have been used to examine the effect on the stability of emulsions. Since the main goal was to develop an ideal stabilization technique for the proposed material mixture, initially no gel was introduced to the system to maintain a simple system with minimized extra influence on the physical behavior. Any other stabilization attempt than particle stabilization (aka Pickering emulsion stabilization) failed to function for a long enough time period to survive the drying process of the emulsion.

Both long tailed and compact conventional surfactant molecules were shown to be inadequate for the stability of the emulsion system prepared here (Figure 4.3, 4.4 and 4.5).

Droplet formation upon shear and phase separation have been observed in micro-scale under optical microscope. The results show that, at the very instant of exposure to shear, all emulsions yield to spherically shaped internal phase aqueous KCOOH droplets suspended in the continuous SBS copolymer solution medium. When no stabilizing agent is used however, the aqueous droplets immediately merge after shear stress terminates. A few drops of the mixture of KCOOH (aq) in SBS medium has been observed under optical microscope after being deposited on a glass slide. (Figure 4.3a). The unstable internal phase droplets swiftly merge upon slightest collusion and yield phase separation. The internal phase occupies ambiguously shaped large sections within hydrophobic polymer solution phase. After drying upon evaporation of the solvent within continuous polymer phase along with the water in the hydrophilic phase, two distinctly separated mediums are left on the glass slide (figure 4.3b). These heterogeneously separated leftover mediums are crystallized KCOOH salt after evaporation of its aqueous medium and solid SBS copolymer casting. (Figure 4.3 b)

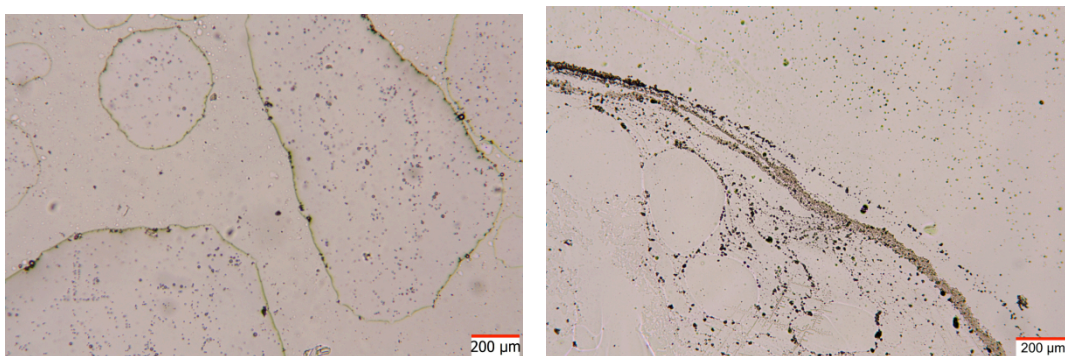


Figure 4.3 Emulsion of KCOOH (aq) within SBS polymer solution, without stabilizing agent a) wet state and b) dry state. The figure shows that the attempt to maintain a stable emulsion without any additional agent has failed.

Next, SDS surfactant material was used to test its effect on emulsion stabilization. SDS requires ionization of its sodium group to yield a negatively charged head, thus a polar material, to function as a surfactant. Therefore it has to be dissolved in water. It was added into the aqueous phase along with KCOOH before the internal phase was emulsified within the hydrophobic polymeric phase. Introduction of SDS into the system has yielded stabilization of the wet emulsion to some extent. However, spherical shape of the droplets were not prevalent. (Figure 4.4a) Droplets with irregular shapes were formed, where these were not stiff and durable enough to survive the drying process without merging. Dry membrane consisted large chunks of KCOOH domains that were not dispersed evenly. (Figure 4.4b)

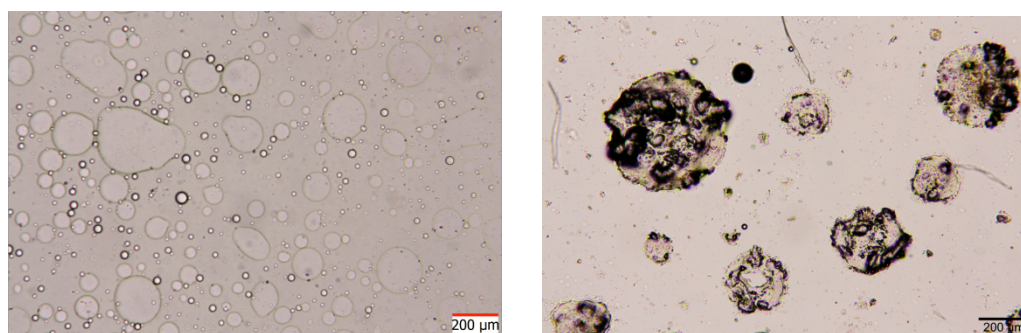


Figure 4.4 Emulsion of KCOOH (aq) within SBS polymer solution, with SDS surfactant as the stabilizing agent a) wet state and b) dry state

As a second approach to stabilize the functional emulsion, emulsification has been tested with PMS. Despite the presence of three methyl groups in its structure, PMS molecule is water soluble. Therefore it is not miscible with the hydrophobic polymer phase. Similar to the preparation procedure of emulsion with SDS, PMS was added into the internal aqueous phase before it was added into the continuous medium. The stability of the resultant emulsion was improved compared to the emulsion with no stabilizer agent, but stability observed with SDS surfactant was still superior to the condition obtained with PMS (Figure 4.5a) The dry membrane obtained upon templating the emulsion on a surface yielded inhomogeneous distribution of KCOOH domains which are observed as gray dispersions (Figure 4.5 b)

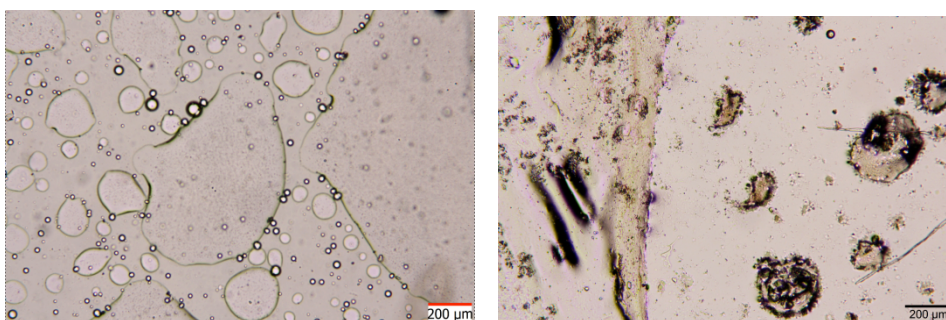


Figure 4.5 Emulsion of KCOOH (aq) within SBS polymer solution, with PMS as the stabilizing agent a) wet state and b) dry state

As a final approach, particles are introduced to the continuous phase prior to emulsification in order to obtain robust and stable emulsions in this study.. Unlike conventional surfactant molecules, solid particles were adequate to maintain well dispersed spherical droplets of the internal aqueous phase and substantially unadulterated functional domains. (Tables xyz – xyz) This demonstrated the superiority of the particle stabilization technique over conventional surfactants. Particle self assembly around the droplets has the

advantages of being irreversible and energetically more favorable over assembly of surfactant molecules.

In figure 4.6, the phase preparation or emulsion phenomena can be seen for different conditions of emulsification with the two immiscible phases. In all the cases studied, SBS polymer solution in cyclohexane was introduced into the aqueous KCOOH solution in identical volume fractions. When no stabilizing agent is used, the aqueous phase disturbed the polymer phase by interfering with the SBS-cyclohexane solution. Water in the internal phase penetrated through the SBS solution and hindered the SBS solubility in cyclohexane. As a result, SBS solution precipitated in cyclohexane. This heterogeneous mixture being less dense than water, suspends above the aqueous phase, leading to the formation of a hierarchically heterogeneous multi-phase mixture. (Figure 4.6 a) Particle stabilization on the other hand, results in the formation of homogeneous, light colored emulsions. (Figure 4.6 b)

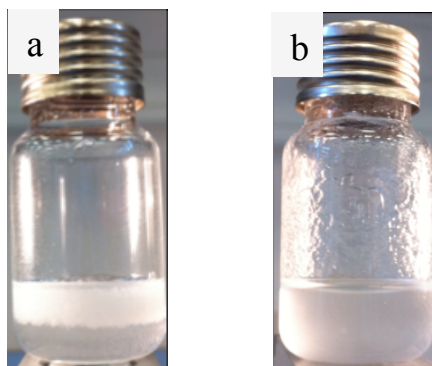


Figure 4.6 The appearances of mixtures of same components, prepared under different conditions a) Without any additional stabilizer agent b) Particle stabilized homogeneous emulsion

The light and semi-transparent color of the particle stabilized emulsion indicates that the internal phase droplets are small enough to avoid scattering of light and are well dispersed.

4.4 Solid Particle Stabilization and Gravity Induced Instabilities

Particle stabilized emulsions acquired for templating in this study were able to stay homogeneous without any form of phase separation for a considerable amount of time. (~1 day) This period of time is sufficient to cast the emulsion and maintain a dry membrane from the template in atmospheric conditions. However, this study has gone further in investigation of the stability behavior of Pickering emulsions even at longer periods of time than required for the primary purpose of templating a membrane.

Over periods of 1 day, regardless of the internal volume fraction or particle concentration, all prepared emulsions underwent a specific type of instability due to gravitational effects. The one homogeneous phase of the emulsion yielded to a lighter colored upper phase and a darker colored lower phase. It should be noted that the absolute phase separation of the system practiced in this study yields a transparent aqueous phase on the bottom and a turbid upper phase above it. The unusual partial separation experienced with particle stabilized emulsions is defined as gravity induced instability (or gravity induced sedimentation). As the solid particle density is the highest of all components in the system, the solid shells tend to sink to the bottom in time. As the particle shells accumulate at the bottom, there appears a phase where they are highly concentrated at the bottom with another phase, which is lighter in color and which has much less number of particle shells within the polymer solution medium. (Figure 4.7) The interactive chemical nature of the modified surface of particles contribute to their approach towards each other.

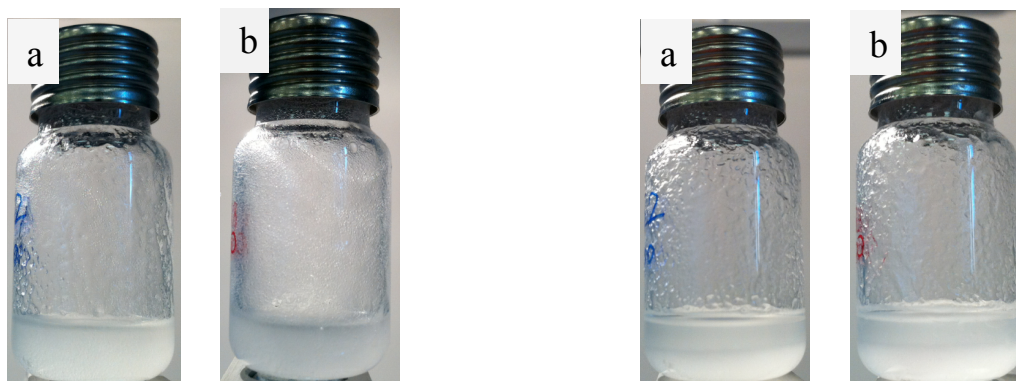


Figure 4.7 Demonstration of gravity induced instabilities in nanoparticle stabilized emulsions. a) 0.17 internal volume fraction and 0.7 % wt nanoparticle concentration b) 0.33 % internal volume fraction and 0.7 % wt nanoparticle concentration. Left couple: Immediately after emulsification. Right couple: After gravity induced sedimentation.

The sediment phase in the bottom consists exclusively of the particle covered internal phase droplets. Thus, as the internal volume fraction increases the volume (thickness) of the sediment phase at the bottom increases.

Accumulation of particle shells do not induce destruction of the self assembly of particles around droplets, as can be observed under optical microscope. (Figure 4.8) Although more closely packed, spherical droplets stay inert against merging and maintain their individual shapes. Thus, such gravity induced sedimentation differs from a total phase separation (Figure 4.3a) as the sediment phase contains both the continuous phase and the internal droplets at the same time, rather than only one phase .

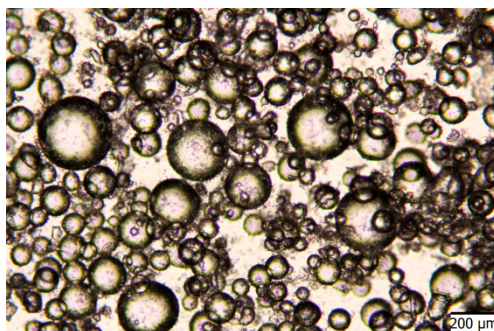


Figure 4.8 Gravity induced sediment phase of an emulsion stabilized by nanoparticles.

4.5 Casting Emulsion Templated Membranes

4.5.1 Morphological Characterization

In order to examine the changes in morphologies of the emulsions during templating, optical micrograph images are obtained for the membranes synthesized with different conditions of emulsions. After placing a few drops of each type of emulsion on the glass slides, they are observed under the microscope in both wet and dried states. . The morphology of both wet and dry castings were found to be dependent on the constituents of the dispersed phase. The effects of particle concentration in the emulsion, internal phase volume fraction, and gelation of the internal phase on the morphology of membranes in both wet and dried states have been studied.

4.5.1.1 The effect of Gelation

Gelation of the functional beads with agarose contributed greatly to stabilization and the homogeneity of the dispersed phase. In order to determine the contribution of various compositional parameters, gelled and non gelled internal phases of the emulsion samples

were prepared, and the effects of internal volume fraction and particle concentration on membrane morphology have been studied. Both wet and dry states of the emulsion template membranes were observed. Dry domains were slightly smaller but comparable in size to their initial wet droplet phase. Gelation of the internal phase yields much denser and stiff droplets within the emulsions, which influenced both the size and the shape of the functional domains. Figure 4.9 displays the difference caused by the gel phase in the wet emulsion droplets right after being placed on the glass substrate. The aqueous gel droplets which contained aqueous KCOOH were larger and much more predominantly shaped than the ones which had solely aqueous KCOOH (without gel). Furthermore, the droplets which did not contain any gel had a tendency to merge and lose stability by forfeiting their spherical shapes, especially when particle concentration is low (0.7 % wt of particles) (Figure 4.9a). It can be observed from figure 4.9b that the gel cores remained stable. The enhanced stability of the internal phase of gel emulsions can be attributed to the defined spherical shape of the dispersed droplets.

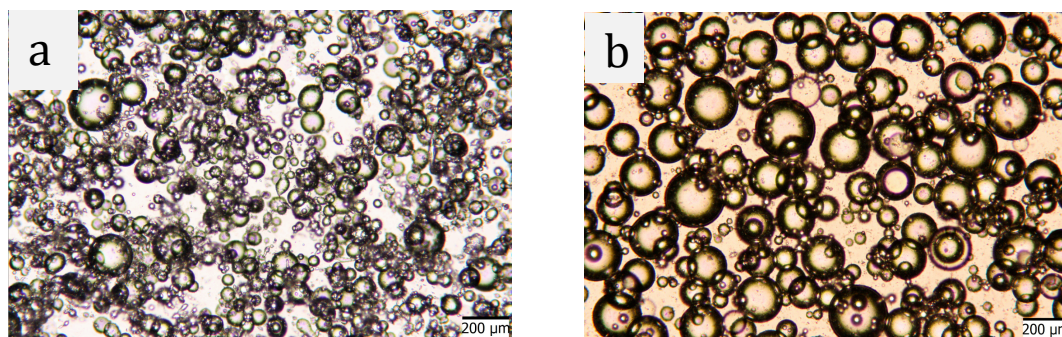


Figure 4.9 Micrographs of the wet emulsion with 3 % internal volume fraction and 0.7 % wt nanoparticle concentration. a) Droplets without agar gel. b) Droplets with agar gel. Scale bar is 200 μm .

The effect of gelation of the internal phase in the wet state of the emulsions are reflected on the dry membranes which are resulted after templating. As can be observed in Figure 4.10a,

the domains without gel phase fail to sustain their spherical shapes after drying. The gel domains on the other hand, have preserved their three dimensional shapes in a large extent, despite having been slightly distorted due to volume change of the continuous phase during drying (Figure 4.10b). Furthermore, the gel core within the domains protect the gel droplets from cracking, and they remain resistant against the capillary pressure effects, which occur during evaporation of the solvent in both phases. The elimination of cracks allows for better protection of the anti-icing agent, which was incorporated within capsules. A crack-free shell around the functional domains is highly desirable, as this would contribute to the stability of the membrane as a whole, which may further allow for better controlled release profiles of the functional agent from the gel domains towards their surroundings.

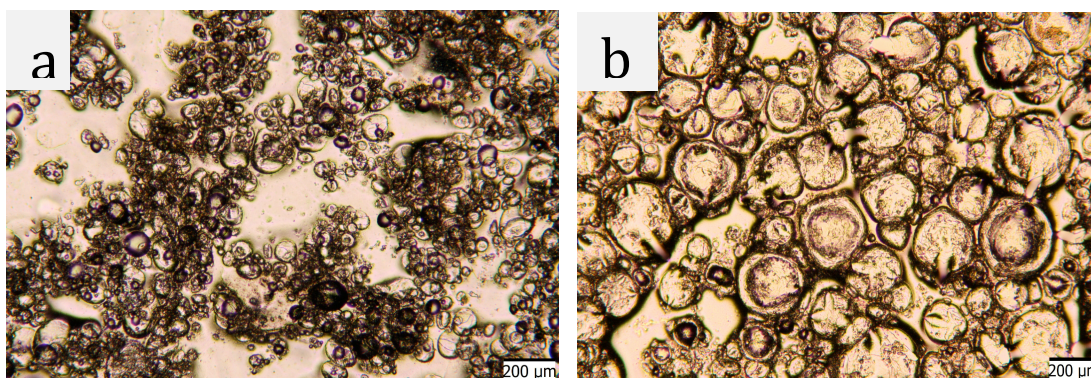


Figure 4.10 Micrographs of the templated membranes after drying of the wet casts displayed in Figure 4.9 a) Domains without agar gel. b) Droplets with agar gel. Scale bar is 200 μm .

It can be observed from figures 4.9 and 4.10 that gel cores have a tendency to be larger in size, however it should be noted that examination of the effect of internal phase gelation for a single sample is not sufficient. Therefore, the effect of gelation is investigated under

different internal volume fraction and particle concentration conditions. Other parameters have apparent influences on stability and morphology of the samples as will be demonstrated in further sections.

4.5.1.2 Particle Concentration Effect

The intended function of nanoparticles for the emulsion templates prepared in this study has primarily been the stabilization of the emulsions for a long period of time such that homogeneously distributed functional domains in the final membrane could be obtained. The stabilization effect of particles is better distinguished in the samples where there is no gel structure in the internal phase, since gel cores remain stable at all nanoparticle concentrations used. In the gel samples, the stability and spherical shapes of the emulsion droplets and templated domains are enhanced significantly regardless of the nanoparticle concentration. In addition to the contribution to stability of emulsions, nanoparticles have effects on gel droplet size and on the bridging behavior between stable droplets.

As particle concentration increases, the droplet size decreases significantly in wet emulsions. Figure 4.11 displays the template gel emulsions of identical internal phase volume, where nanoparticle concentrations were changed from 0.4 to 1.0%. It should be noted that the particle concentration referenced here is not the concentration in the final emulsion form. It is the particle weight (in mg) per cyclohexane volume (ml) before the addition of polymer solution.

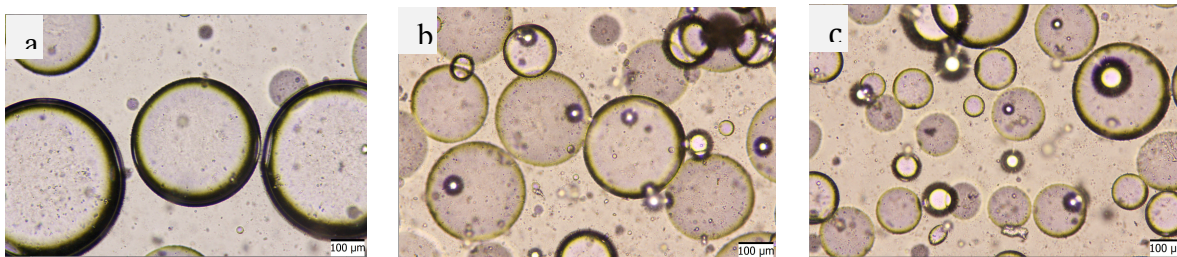


Figure 4.11 Micrographs of wet emulsions with gel droplets, 0.1 internal volume fraction and particle concentration of a) 0.4 % b) 0.7 % c) 1.0 %.

As can be deduced through comparison of Figures 4.11 a, b and c, low internal volume fraction (0.10) along with reduced particle concentration leads to the formation of giant (200 – 400 μm) functional domains (Figure 4.11 a). This has most probably occurred as a result of the energy favor of full coverage of droplets in the emulsion. The particles in the system tend to minimize the interface area between the continuous polymer phase and the aqueous gel phase. However, full coverage requires reduction in the surface area of functional droplets, thus increase in their size. The supportive gel structure further contributes to the enlargement of emulsion droplets. As particle concentration increases, greater interfacial area, accompanied by smaller droplet size and greater number of droplets per unit area were obtained (Figure 4.11 b and c). This effect of particle concentration on droplet size has also been reflected on the templated dry membranes. The giant droplets surrounded by the particles of 0.4 % have yielded similarly large dry domains. (Figure 4.12 a) At lower particle concentrations, the large domains tend to come in contact to form particle bridges by sharing particles among shells. This bridging compensates insufficient number of particles per droplet and contributed to the attempt of maintaining fully covered spheres.

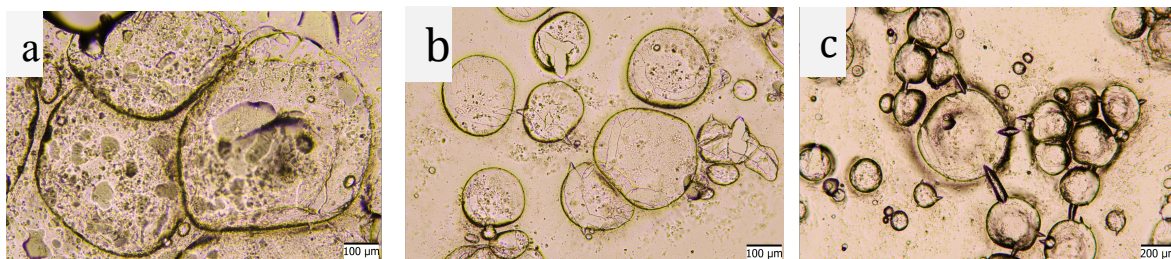


Figure 4.12 Micrographs of emulsion templated dry membranes consisting gel cores, 0.10 internal volume fraction and a) 0.4 % wt. particles b) 0.7 % wt. particles c) 1.0 % wt. particles.

The gel domains do not sustain the droplets' perfect spherical shapes. Nevertheless they remain stiff enough to maintain a three dimensional closed shape.

4.5.1.3. Internal Volume Fraction Effect

The two most significant effects of increasing the internal volume fraction are on size and the fraction of surface covered with functional domains on the polymeric membrane.

Authors??.. et al reported that increase in internal volume fraction was accompanied by increase in droplet size. Contrary to this finding, fractional increase of internal volume in this study had an indirect effect on droplet size in wet emulsion. Larger internal volume fractions resulted in the formation of smaller the droplets (Figure 4.13) This contradictory phenomenon is attributed to the method of emulsification used in this study. Unlike the mixing methods used in the literature (sonication), vortexing has been employed to mix the two separate phases namely, the continuous polymer solution and the dispersed aqueous KCOOH. Vortex causes high shear within the viscous medium. Therefore, the dispersed droplets collide onto each other with high energies. Such collisions cause fractionation of the spherical droplets. The increased viscosity which results from larger fractional volume of droplets will yield higher shear between them.

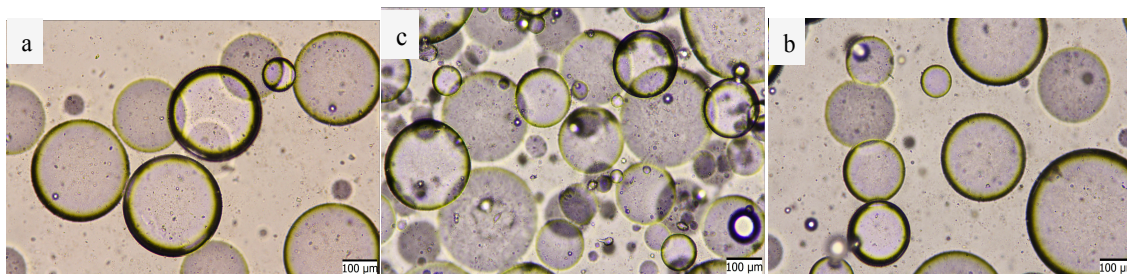


Figure 4.13 Micrographs of wet emulsions with gel droplets, 0.7 wt. % particles and internal volume fraction of a) 0.10 b) 0.17 c) 0.33

The second predominant effect of fraction of droplets within emulsion is the surface coverage of functional domains on the membrane. As anticipated, the more fraction of internal phase there is in the emulsion, the more area on the membrane is occupied by the functional droplets. (Figure 4.13)

It should also be noted that increased internal phase fraction results in increased contact of droplets in wet state and more contact between domains on dry membrane. Unlike the case where domains come in contact under low particle concentration conditions, the contact caused by the internal volume increase is associated to energy favor. It has rather to do with the simple fact that there is not enough space in the continuous medium for the droplets to be dispersed individually as the emulsion shrinks during drying. When the internal phase fraction is high, the SBS polymer base is completely covered packed functional domains. Thus, more internal phase yields to small and compact domains that are slightly deformed due to pressing on each other.

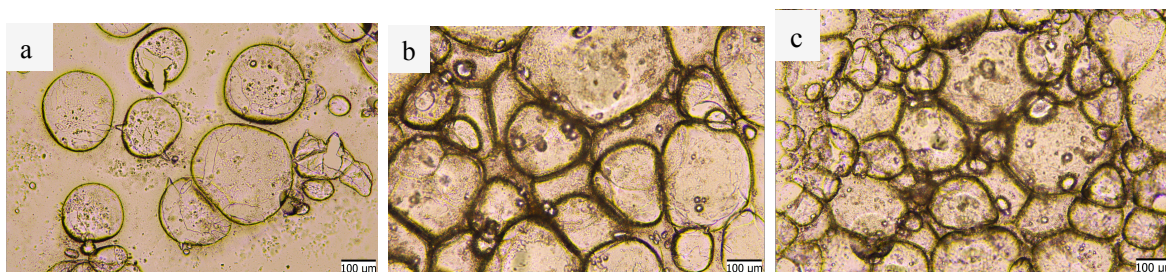


Figure 4.14 Micrographs of emulsion templated dry gel domains with 0.7 wt. % particles and internal volume fraction of a) 0.10 b) 0.17 c) 0.33

4.5.2 Effect of Internal Phase Volume Fraction and Particle Concentration on Average Wet /Dry Droplet Size

The effect of internal phase volume fraction and nano particle concentration on average droplet size have been demonstrated in Figures 4.15 through 4.18. For the case of emulsions prepared by the functional droplets that are not gelled, the average size for wet droplets or dry domains show similar trends against variations in particle concentration and internal phase fraction. The average diameter being smaller in dry samples is simply due to the shrinkage phenomenon which occurs during drying. Increases in the internal phase volume caused smaller sized droplets and smaller dry domains as was mentioned in the previous section. There are two reasons to explain this effect. As the volume fraction occupied by the internal phase increases, the shear rate (or shear stress) which droplet shell surfaces apply to each other increases. Increased shear rate decreases the droplet size. Additionally, droplets tend to get smaller to become close packed in order to ‘fit’ into the limited available space within the continuous medium.

Among the three different particle concentrations, the droplet size maximizes at the median (0.7 %) (Figure 4.15 and 4.16). Both increasing and decreasing particle

concentration from this value causes smaller diameters for droplets/domains. Lower particle concentration is insufficient to stabilize the droplets. Therefore, the internal phase cannot form definitely shaped droplets. Instead, scattered, irregular droplets were observed in the continuous medium. Higher particle concentration on the other hand, is sufficient to cover larger surface area of droplets. Hence, the droplets increase their surface area by decreasing their sizes.

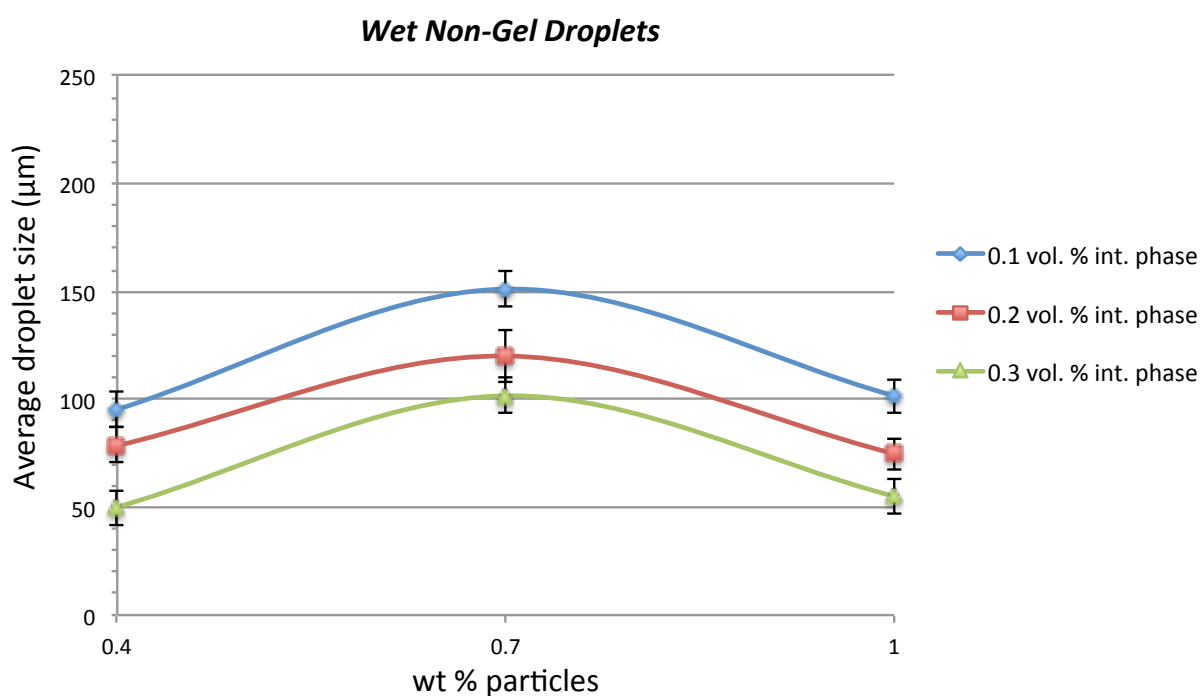


Figure 4.15 Average droplet sizes with respect to nanoparticle concentration for various internal phase fractions in wet emulsion state (without gel).

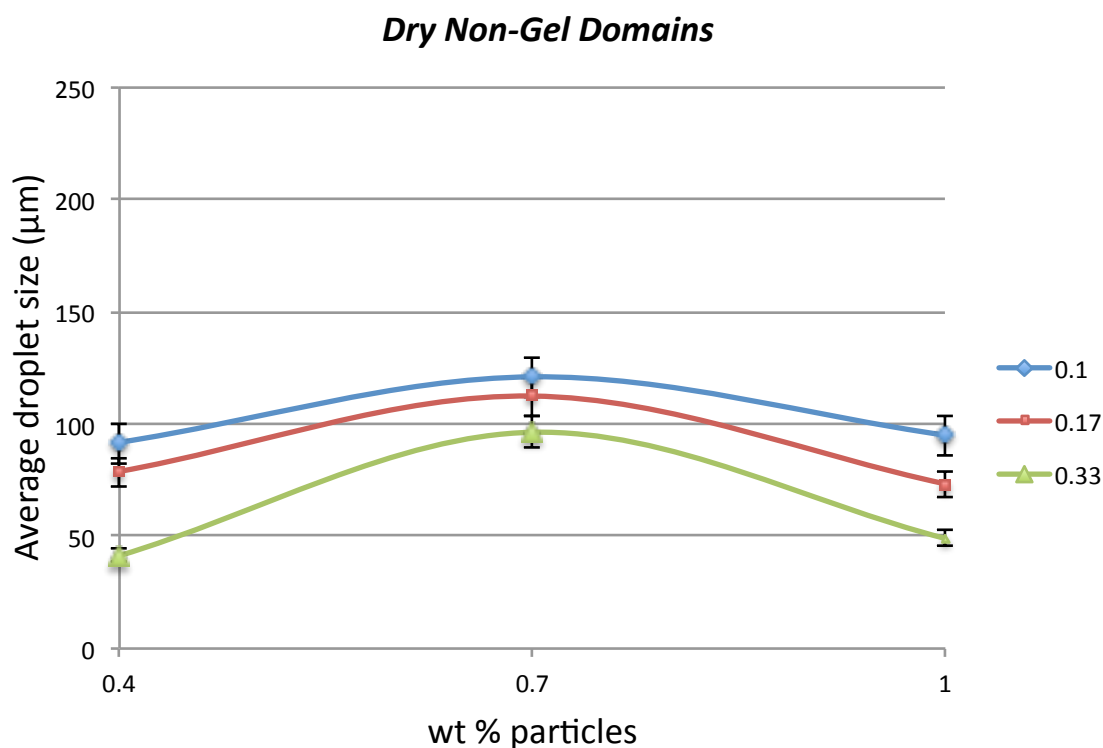


Figure 4.16 Average domain sizes with respect to nanoparticle concentration for various internal phase fractions in dry membrane state (without gel).

Average droplet sizes for both wet and dry states were larger for the gelled internal phases compared to non-gelled cases. Increased internal volume fraction causes smaller droplets to form, due to increased shear among droplets interfaces and spatial hindrance, as was mentioned above. When internal volume fraction was high in gelled samples (0.33), particle variance yielded the same effect as in the non-gelled samples. Lower particle concentration was inadequate to stabilize all internal phase in the shape of spherical droplets. However, for lower internal volume ratios, the gelled samples deviated from the behavior of non-gelled

ones. Due to the intrinsic stiffness of the gel droplets, 0.7 % and 1.0 % particle concentrations were sufficient to stabilize high amount of internal phase into spherical forms. Nevertheless high internal phase fraction induces smaller surface area of droplets. Thus, larger droplets form to allow for the complete particle coverage of droplets. Contrary to the non-gelled emulsion templates, gelled emulsions induced different trends for wet and dry states.

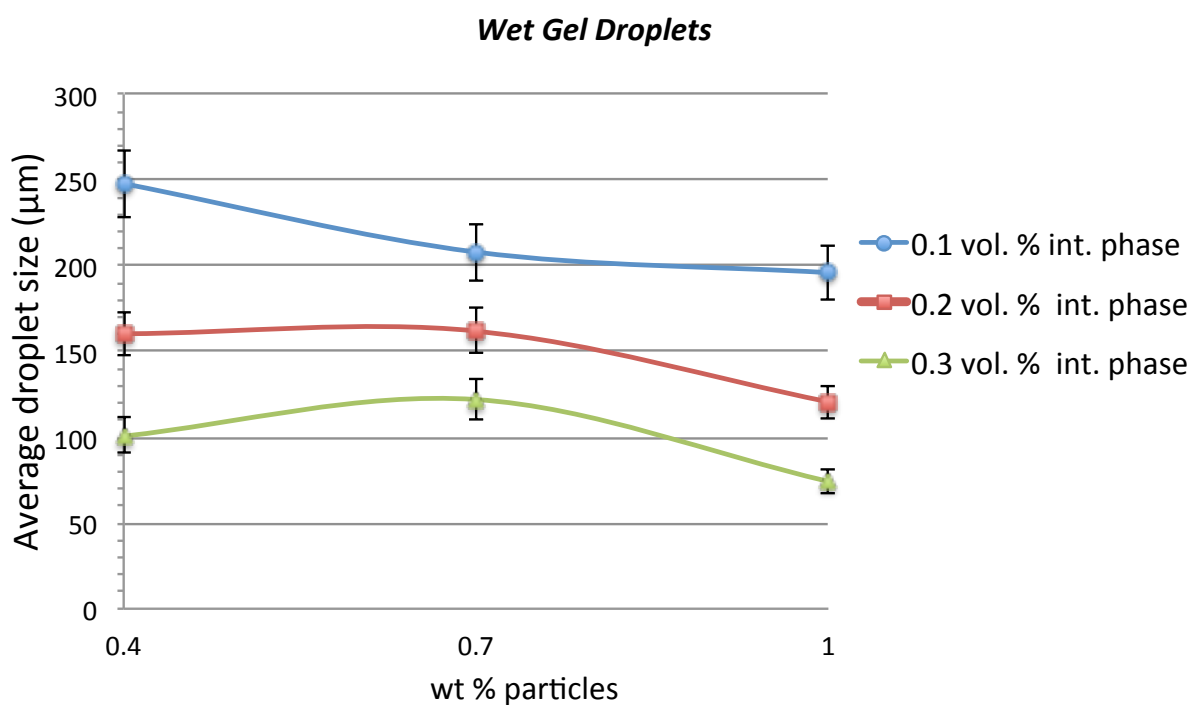


Figure 4.17 Average droplet sizes with respect to nanoparticle concentration for various internal phase fractions in wet emulsion state (with gel).

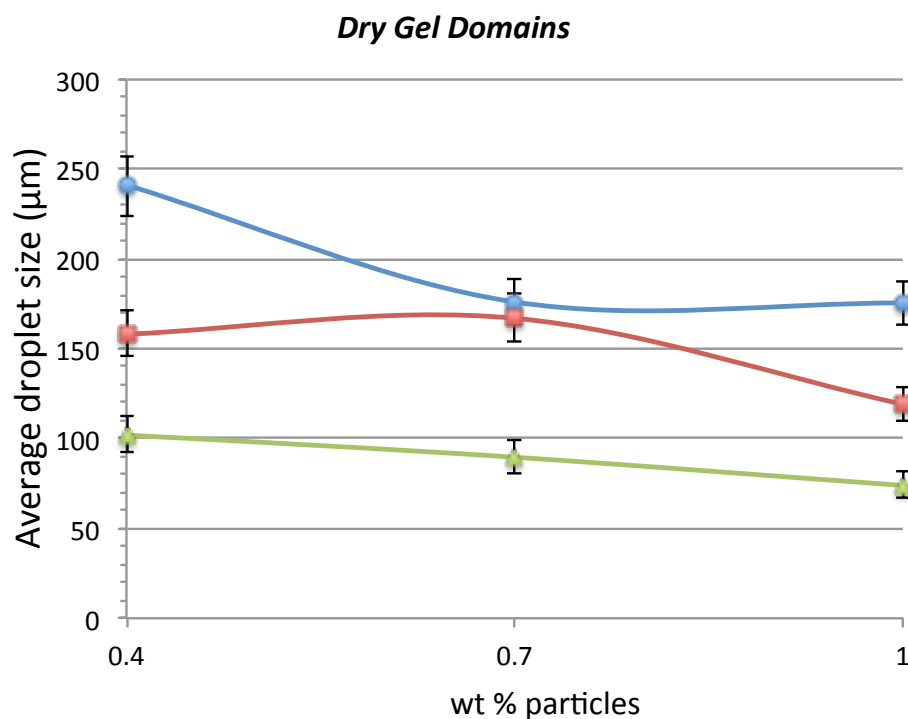


Figure 4.18 Average domain sizes with respect to nanoparticle concentration for various internal phase fractions in dry membrane state (with gel).

The sensitivity of the system to the three parameters considered in this study (e.g. gelling the functional cores, varying internal volume ratio, varying particle concentration) was clearly observed on membrane morphology and average droplet sizes. Different responses to parameter changes were observed in wet and dry states of the membrane. In order to investigate the successive effects of these parameters, several matrices are constructed which display optical microscope images of membranes resulted from three different internal phase ratios, three different particle concentrations and those prepared with both

gelling and non-gelling methods for each combination (Figures 4.XXX through 4.YYY). Furthermore, both wet and dry state average droplet sizes are summarized in Table 4.1.

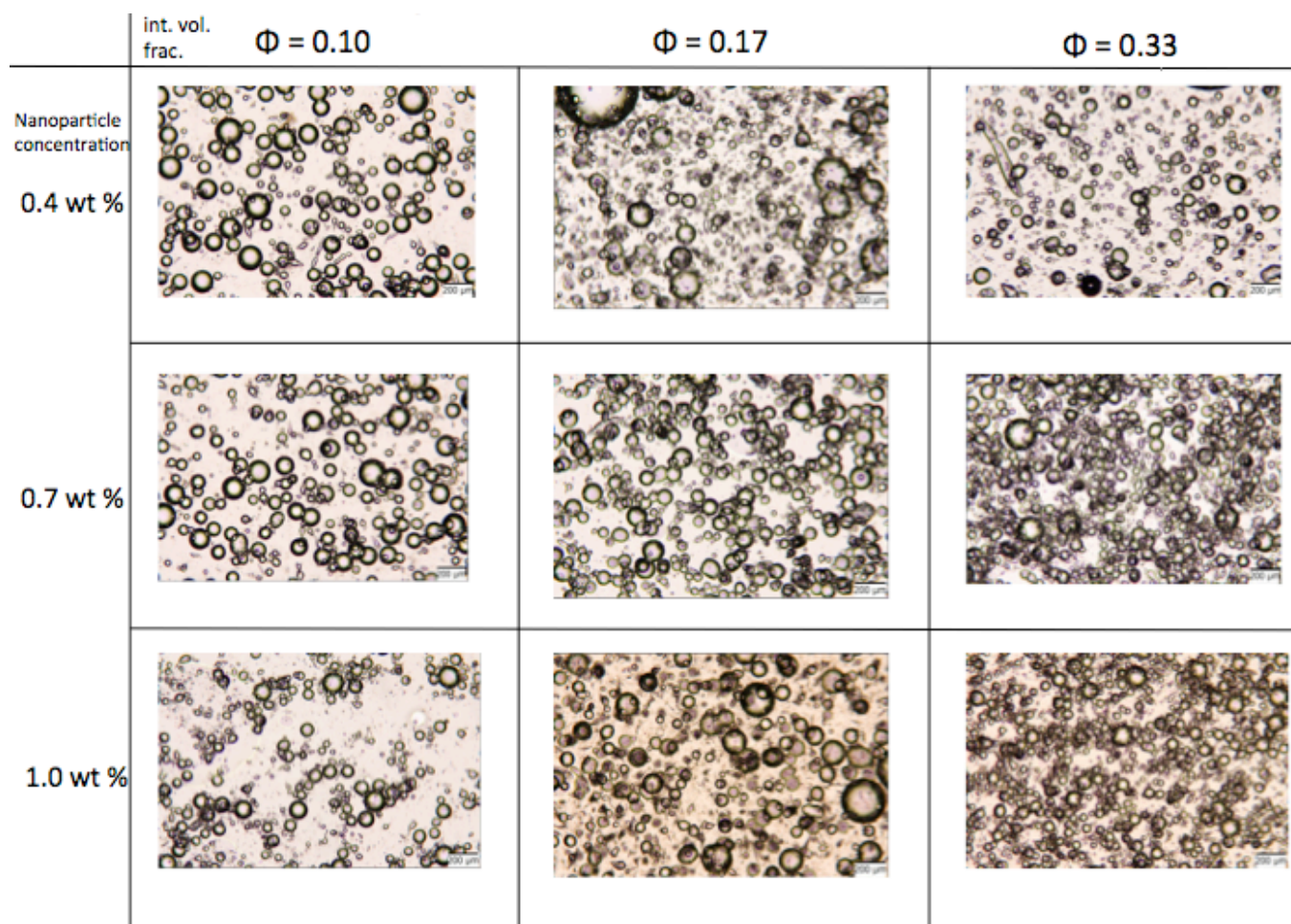


Figure 4.36 Matrix of optical microscope images for wet emulsions without gel cores under magnification with 5x objective.

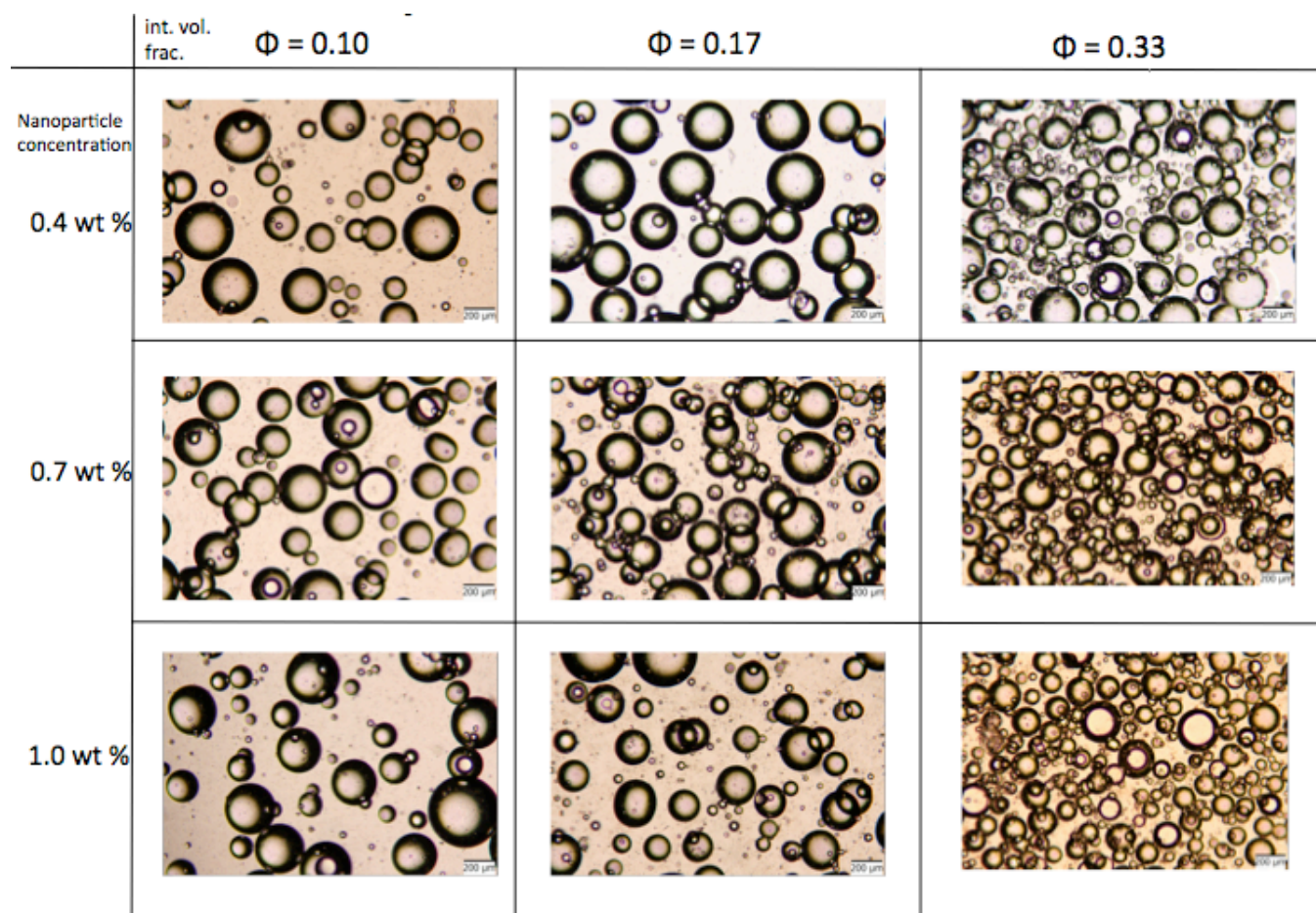
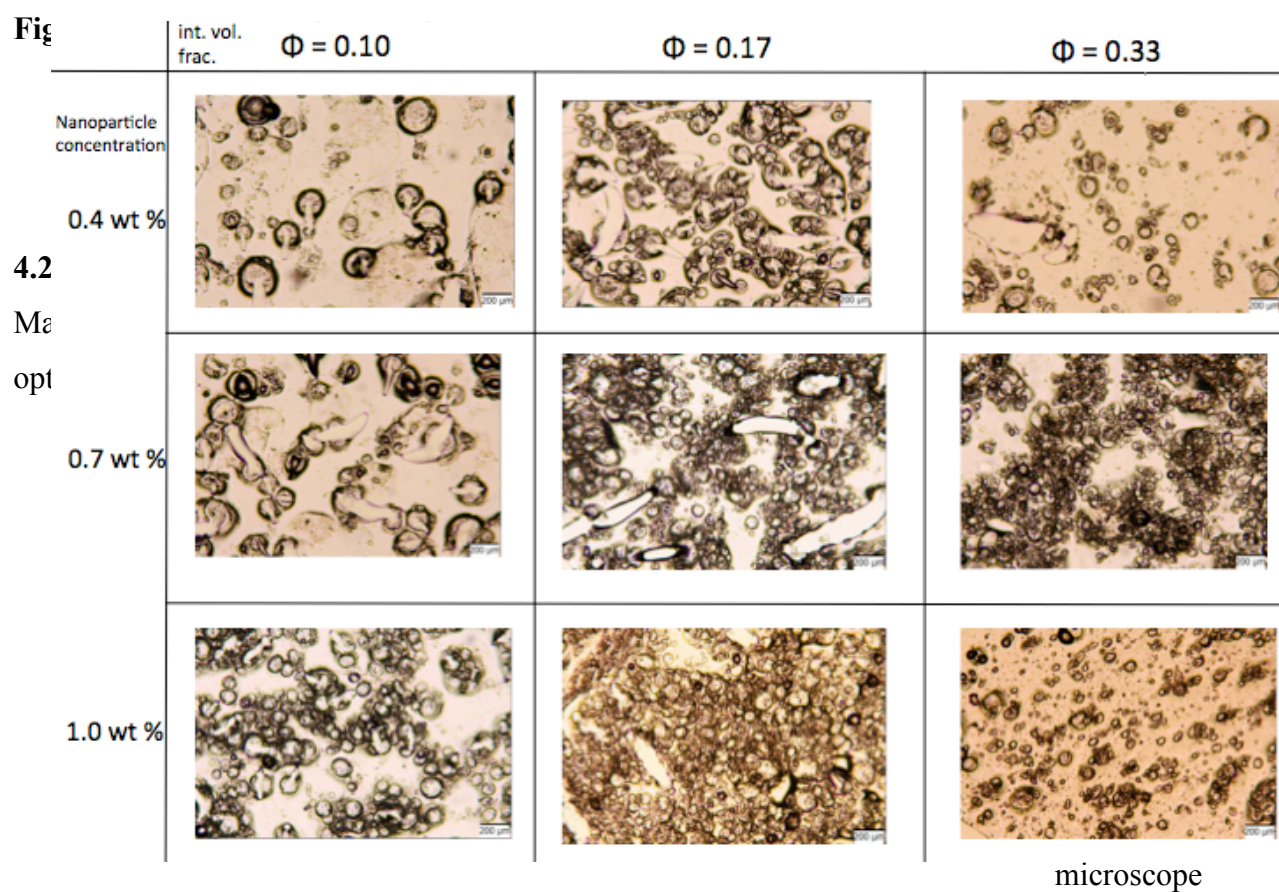


Figure 4.8 Matrix of optical microscope images for wet emulsions with gel cores under magnification with 5x objective.



images for dry emulsions without gel cores under magnification with 5x objective.

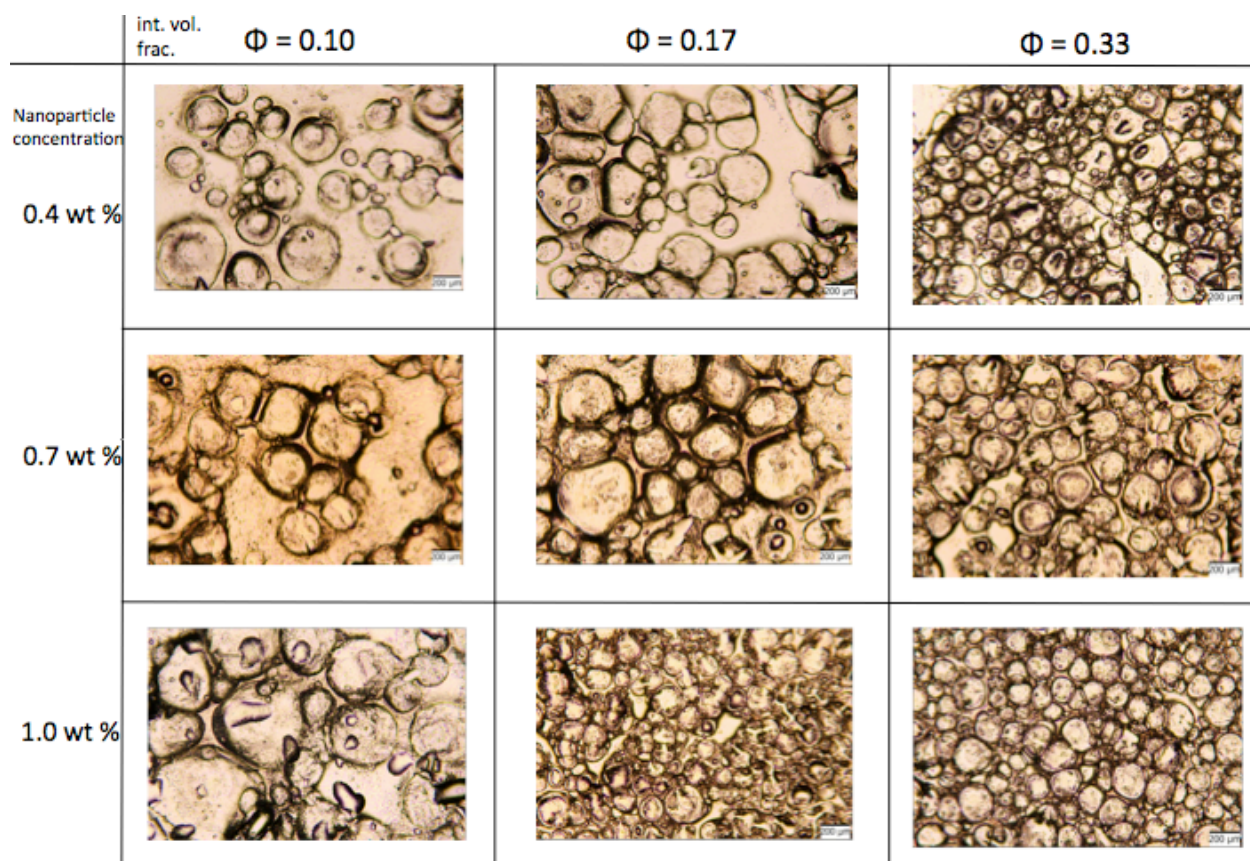


Figure 4.30 Matrix of optical microscope images for dry emulsions with gel cores under magnification with 5x objective.

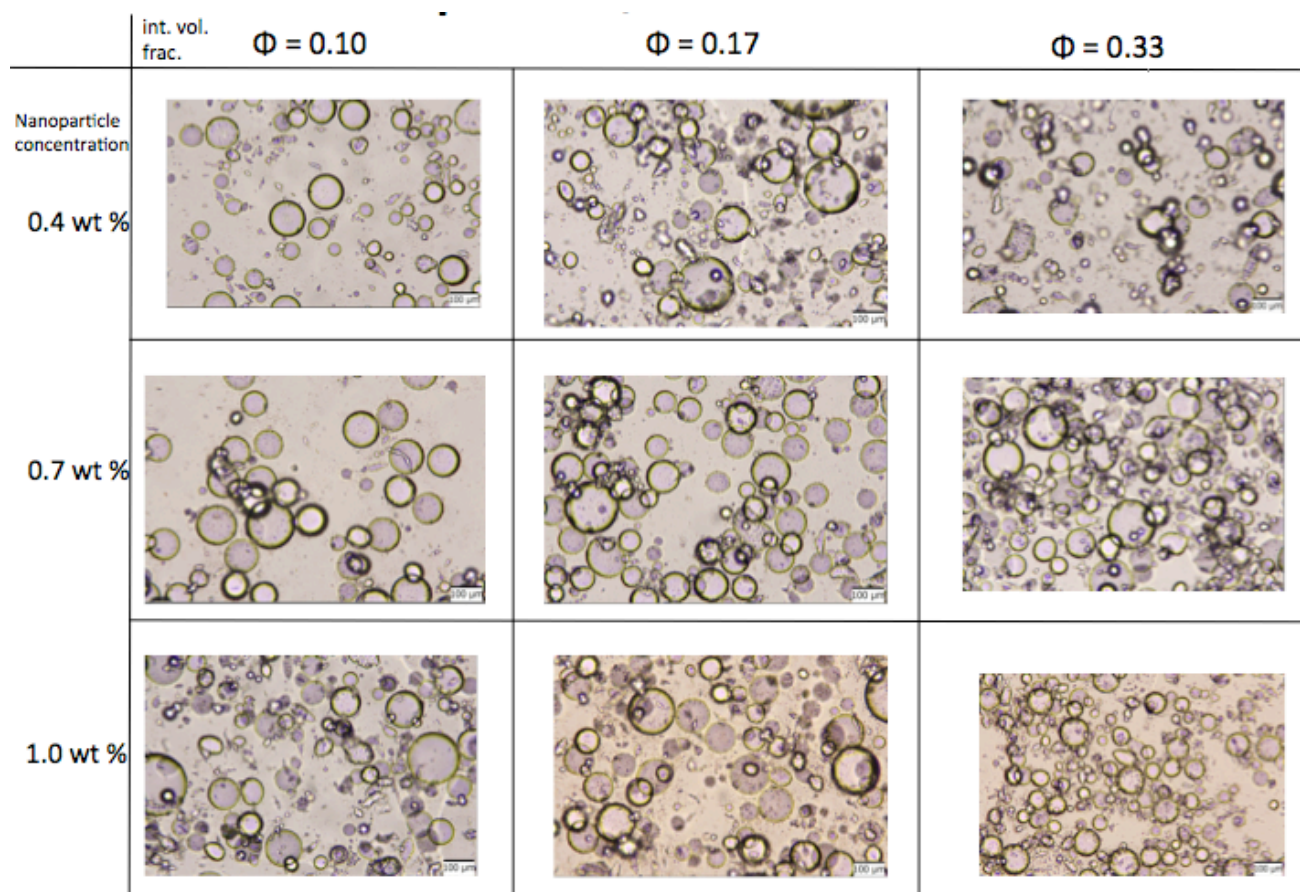


Figure 4.31 Matrix of optical microscope images for wet emulsions without gel cores under magnification with 10x objective.

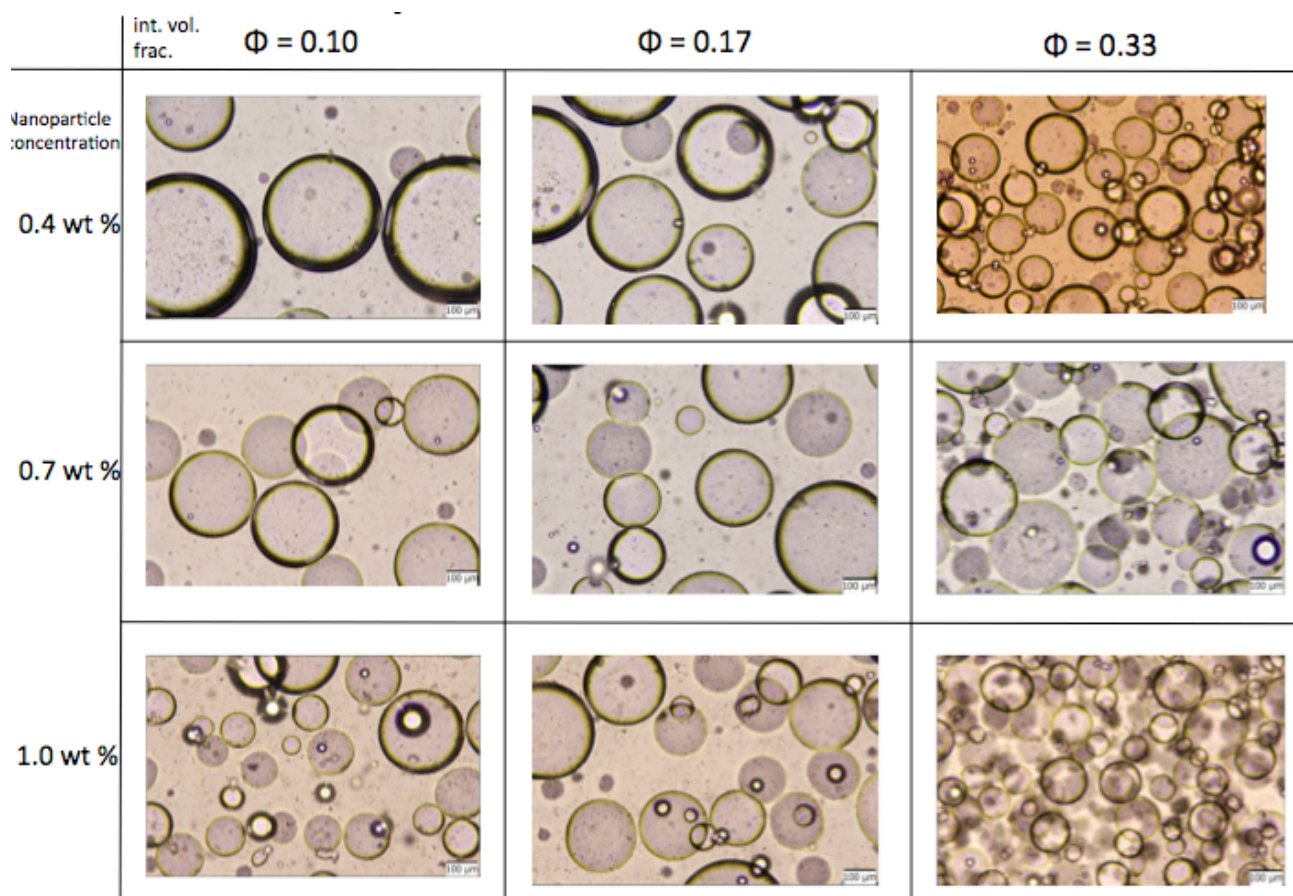


Figure 4.32 Matrix of optical microscope images for wet emulsions with gel cores under magnification with 10x objective.

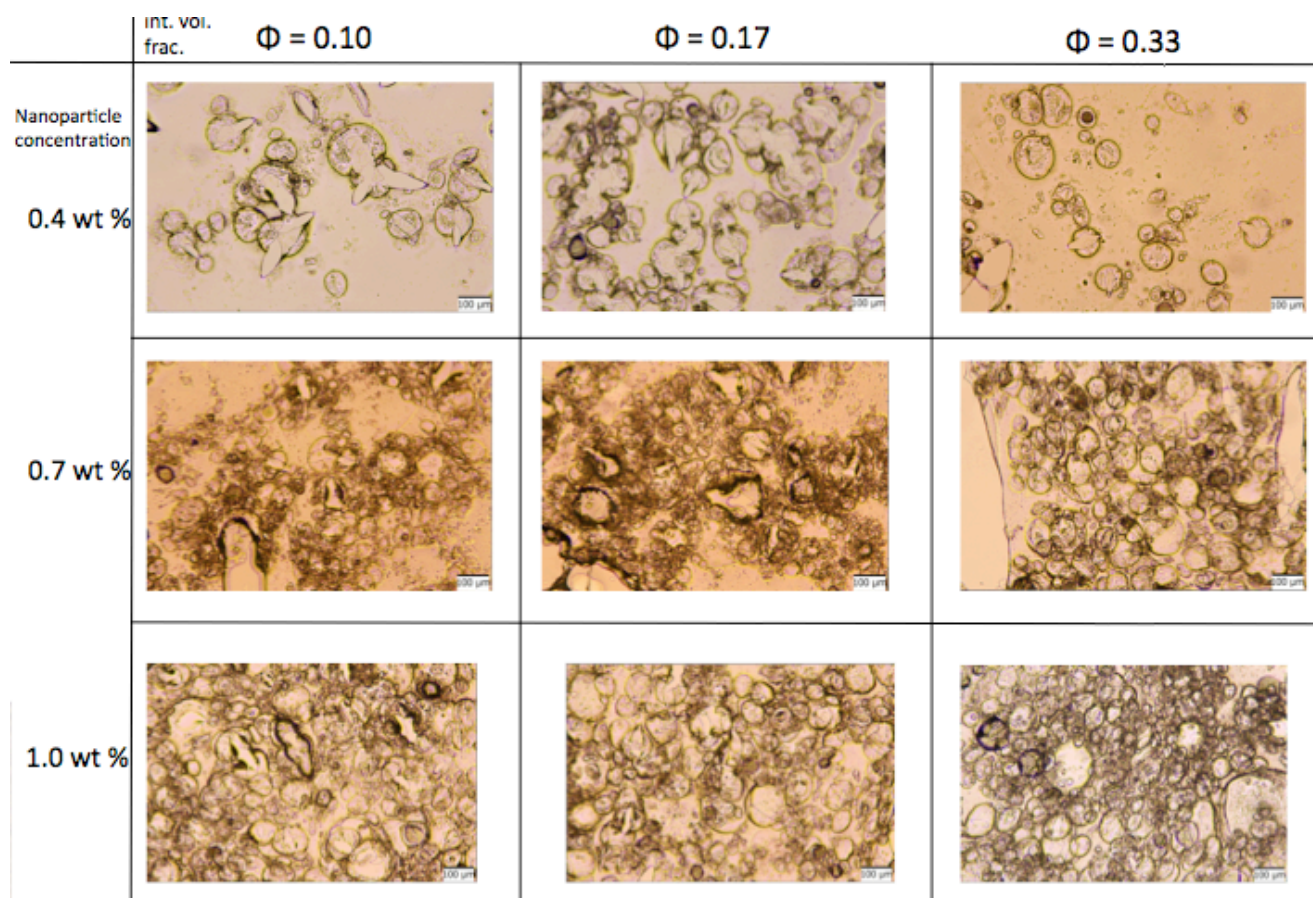


Figure 4.33 Matrix of optical microscope images for dry emulsions without gel cores under magnification with 5x objective.

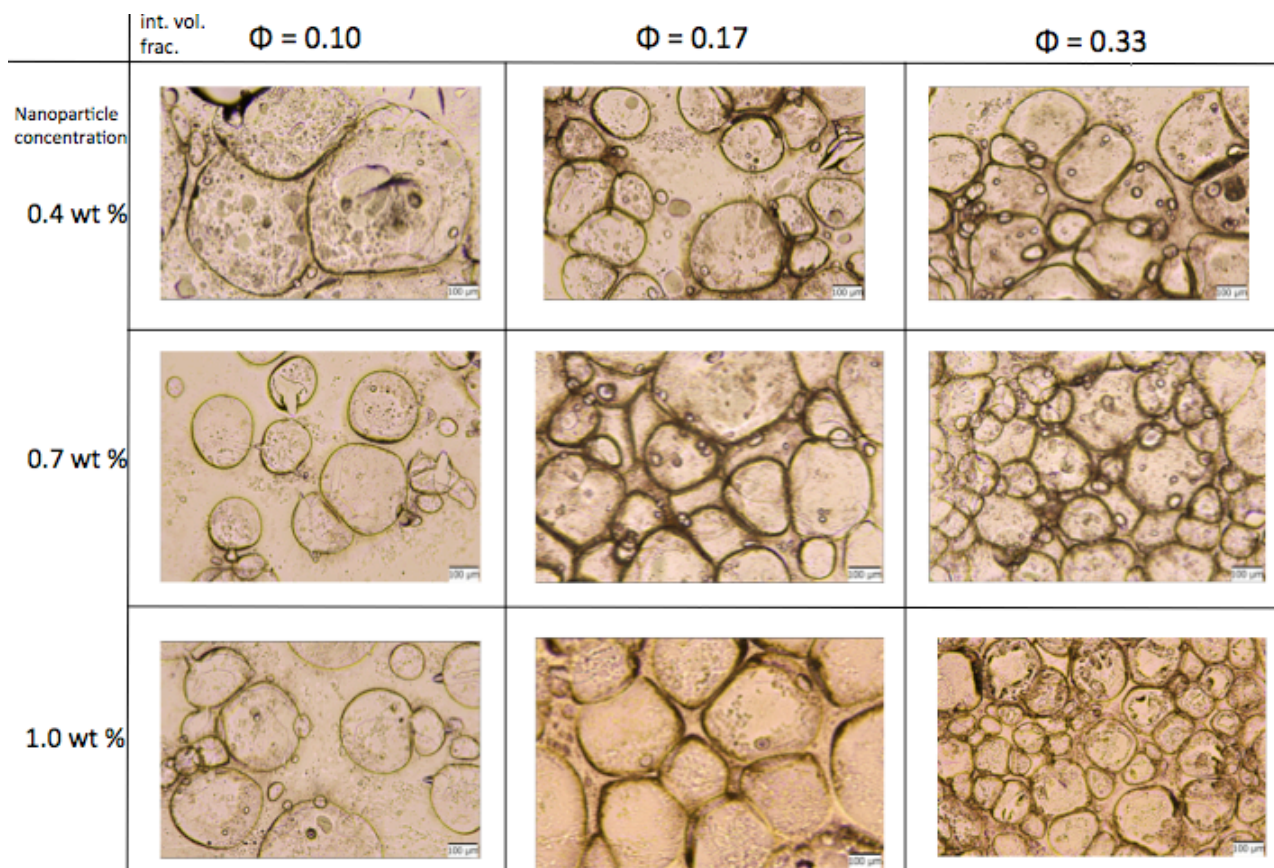


Figure 4.34 Matrix of optical microscope images for dry emulsions with gel cores under magnification with 10x objective.

Figure 4.36 displays the distribution of droplet size with respect to % droplets for wet emulsions formed with 0.17 internal volume fraction and 1.0 % wt. of particles. It is observed from the distribution that gel domains are distributed along a wider range of droplet size, starting from 20 μm and extending up until 300 μm diameter. The size

distribution for non-gel droplets occupies a narrower range although it does not include any droplets of diameter smaller than 15 μm . The figure also shows that, gelation in the hydrophilic phase promotes smaller sized gel droplets, however gel droplets that are bigger than of a 180 μm diameter is more in number than the ones that are smaller. For the case of non gel in the hydrophilic phase, the greatest size a non-gel droplet can reach is 180 μm . The average droplet sizes calculated also agree with this observation that gel droplets tend to maintain greater sizes despite the fact that small gel droplets are possible.

Figure 4.20 demonstrates the distribution of droplet size for wet emulsions formed with 0.33 internal volume fraction and 1.0 % wt of particles. Similar trends were obtained, where the maximum diameter of a non-gel droplet was 160 μm , while gel droplet sizes were spread on a wider range, reaching a droplet diameter of 220 μm . Minimum droplet diameter for both gel and non-gel droplets were 20 μm .

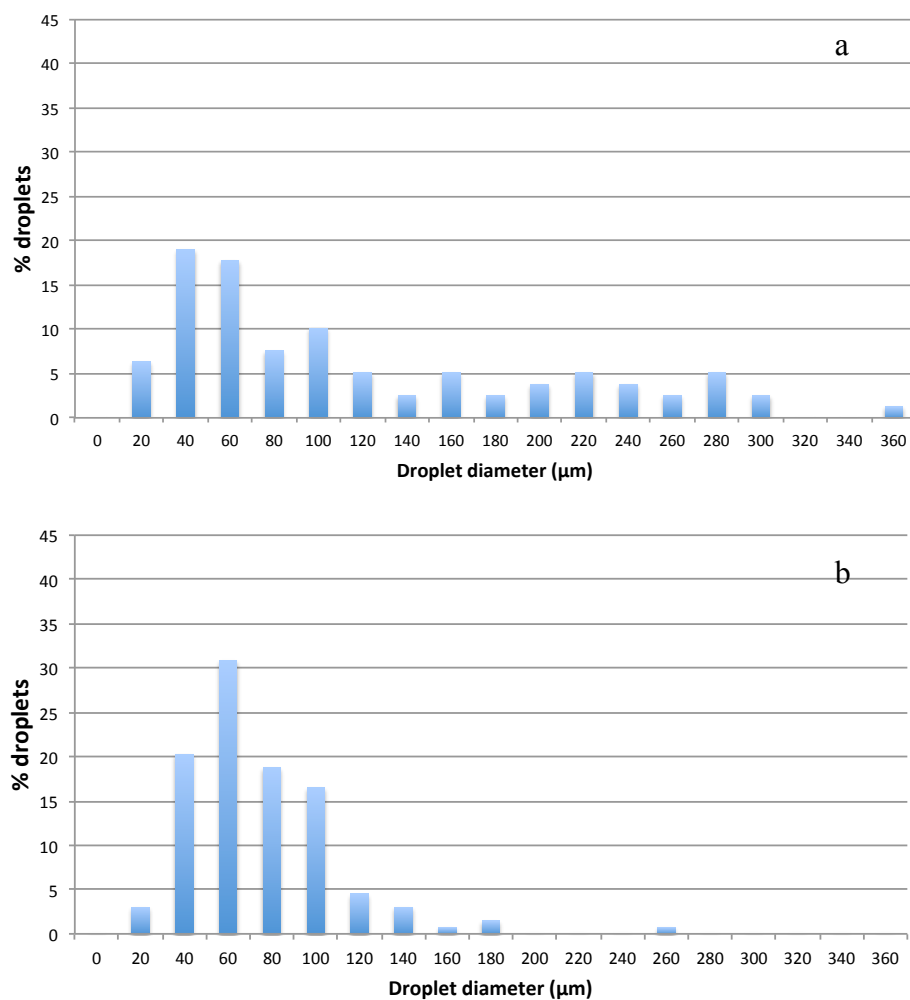


Figure 4.36 Droplet size distribution by fraction for 0.17 int. vol. fraction and 1.0 % wt. particles a) gelled droplets (Average size = 120.65 μm) b) free of gel (Average size = 74.89 μm)

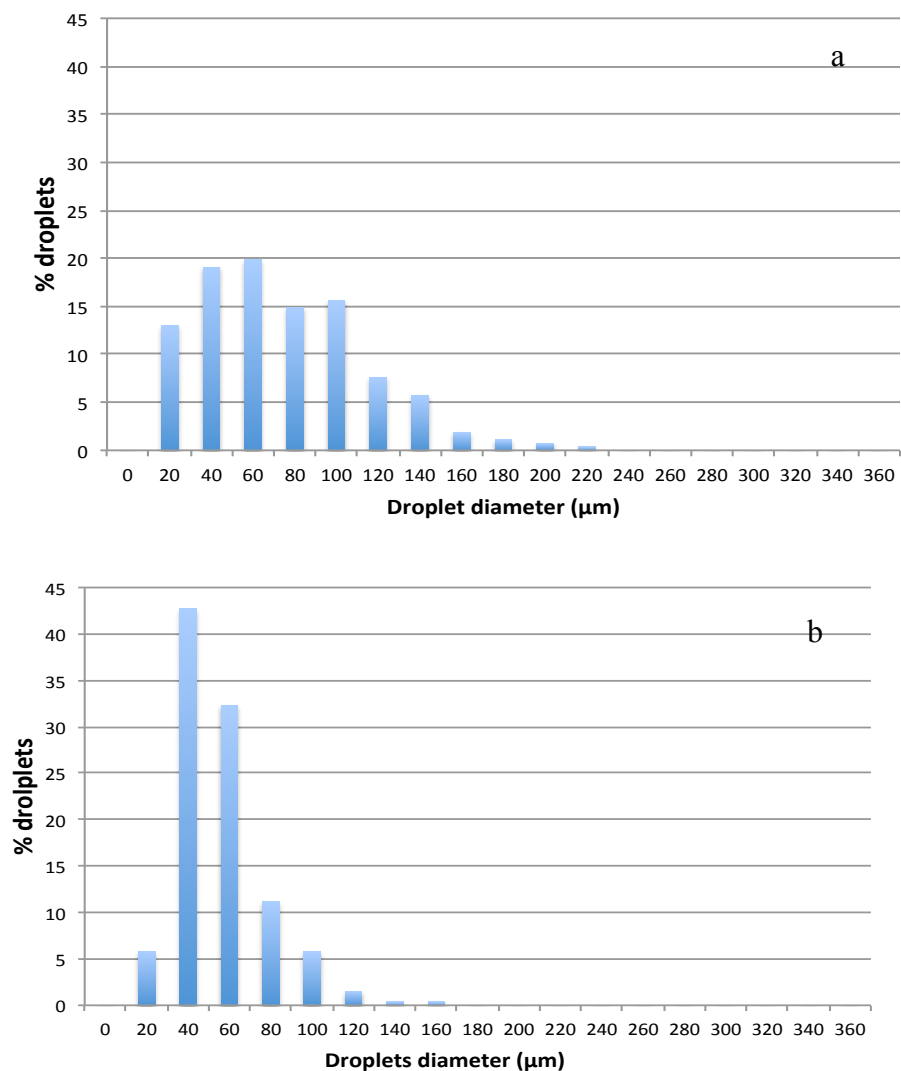


Figure 4.8 Droplet size distribution by fraction for 0.33 int. vol. fraction and 1.0 % wt. particles a) gelled droplets (Average size = 74.3 μm) b) free of gel (Average size = 55.13 μm)

Table 4.1 displays the average wet and dry droplet sizes for all samples examined in this study.

		WET			DRY			
		int. vol. frac ->	0.10	0.17	0.33	0.10	0.17	0.33
		np concent. wt %						
NO GEL	0.4 %	95.25	78.82	49.73	91.24	78.43	41.27	
	0.7%	151.11	120.18	101.67	120.98	112.43	96.37	
	1.0 %	101.65	74.89	55.06	95.17	73.32	49.03	
WITH GEL	0.4 %	248.12	160.26	101.24	240.67	158.65	102.38	
	0.7%	208.03	162.14	122.25	175.98	166.91	89.59	
	1.0 %	196.09	120.65	74.24	175.43	119.07	73.89	

Table 4.1. Average droplet/domain sizes (μm) for all samples in wet and dry states with respect to internal volume fraction (horizontal) and particle concentration % (vertical)

4.5.4. Surface Characterization

The location and morphology of the dry domains embedded within the polymeric membrane base directly determine how KCOOH is distributed within the membrane. The surface behavior effect of this distribution has been investigated through water contact angle (WCA) analysis on the templated membranes. The functionalized polymer membranes in general are slightly less hydrophobic than sole SBS membrane, where WCAs were about 84 °- 94°. Figure 4.29 shows the WCA measurement results for all samples in the range of 0.4% - 1.0% wt. particle concentration and 0.1 – 0.3 internal volume fraction which were not gelled. All contact angles measured for non-gel samples were stable and did not experience a significant variation over time. Figure 4.30a displays the initial and final WCA's of all samples prepared with gel droplets. Some samples among the gelled ones displayed a dynamic contact angle over time due to the presence of higher internal phase and hence higher water absorption capacity by the gel phase.

Figure 4.30b demonstrates one particular group of samples which behaved different from the rest of the samples. The figure shows the comparison of WCA behavior 15 seconds after water droplet deposition on membrane surfaces. Immediately after water droplet deposition on membrane surface, WCA measured were in between 70° - 80° (figure 4.30a). However, for membranes with higher internal phase content (0.2 and 0.3) and at 0.7 and 1% particle concentrations, the droplet was subsequently absorbed by the gel phase of the membrane, which reduced the WCA to ~0° in seconds.

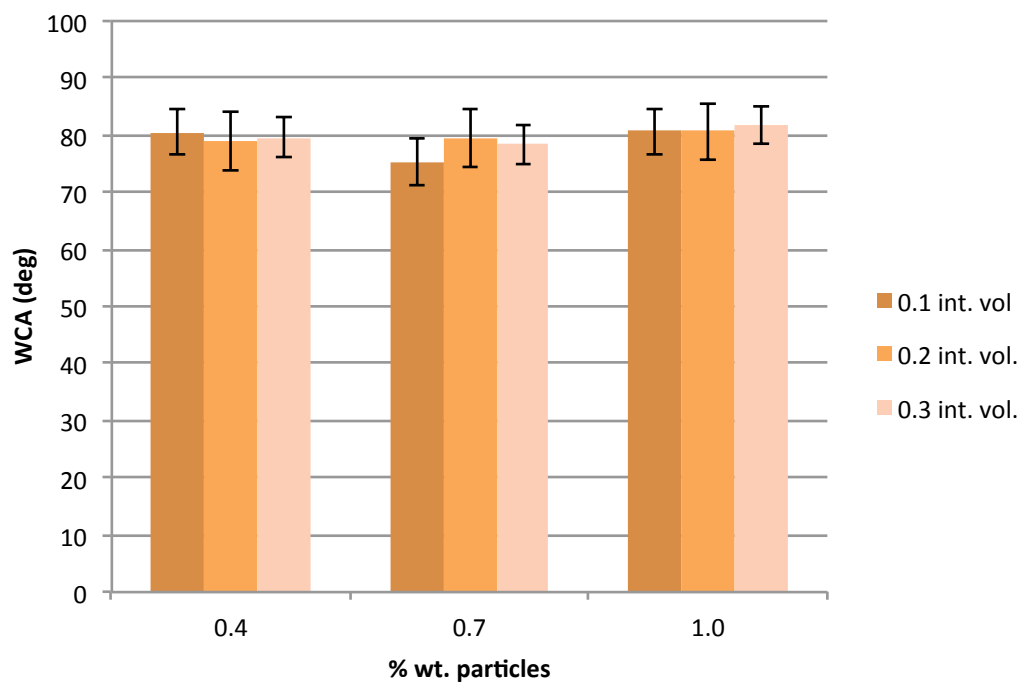
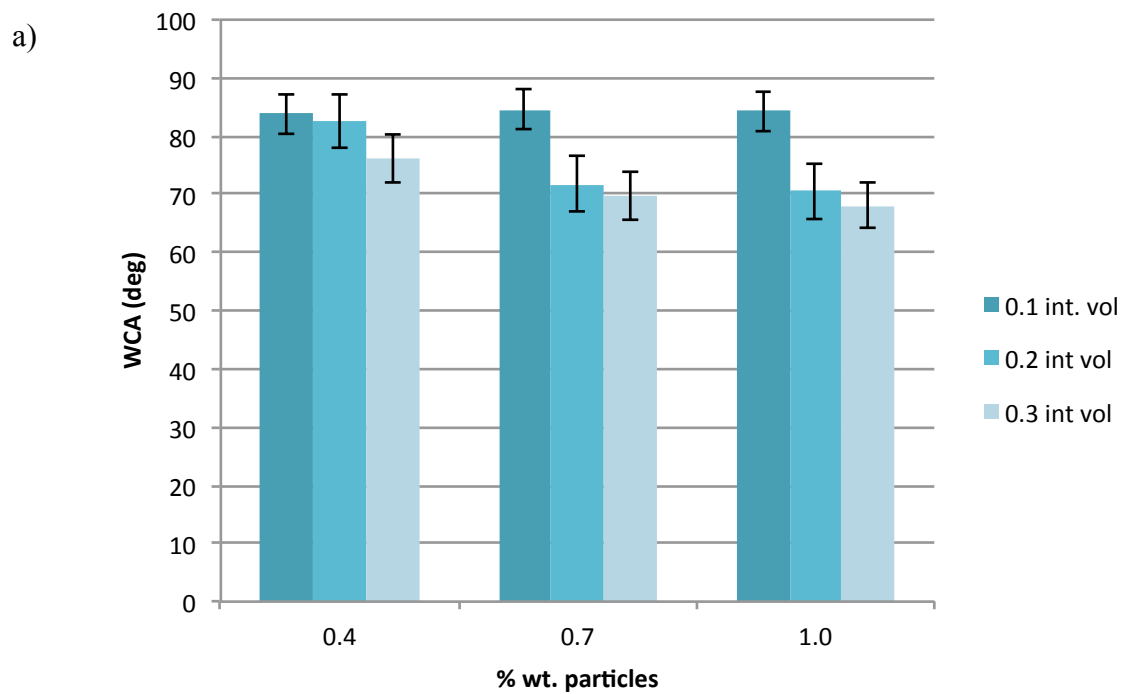


Figure 4.29 WCA ($^{\circ}$) measurements for emulsion templated functional membrane of different compositions without gel. Each series represents an internal volume fraction as displayed in the legend. Horizontal axis represents particle concentration in wt. %.



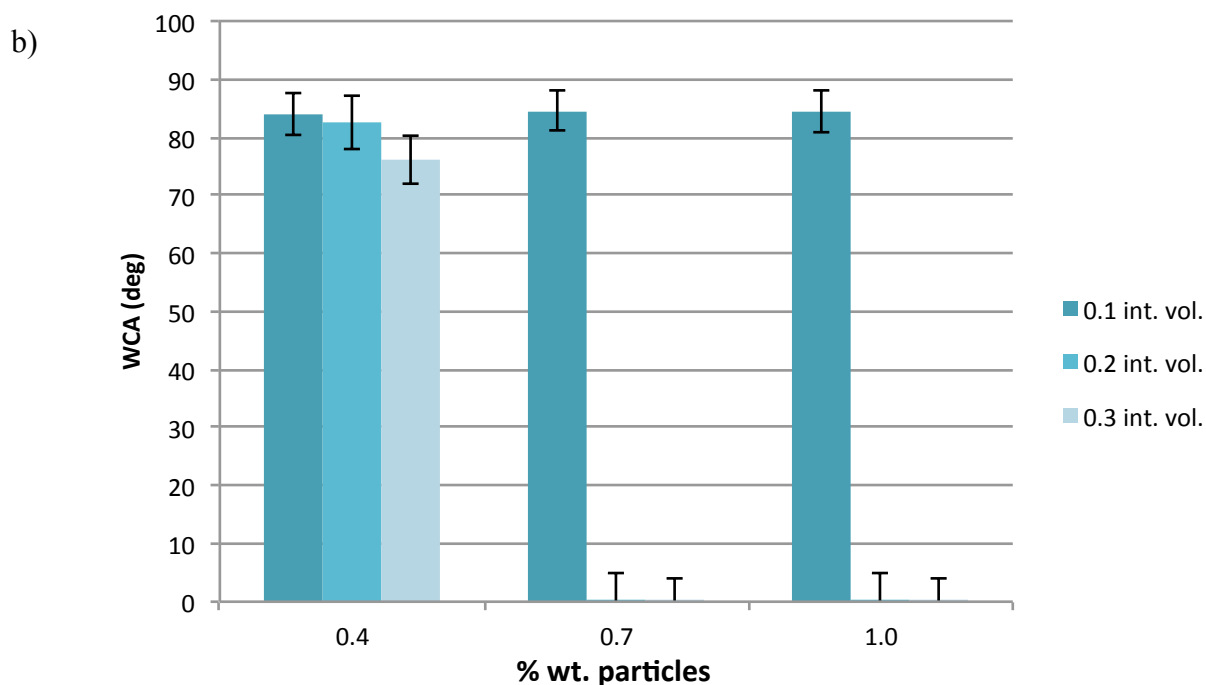


Figure 4.30 WCA ($^{\circ}$) measurements for emulsion templated functional membrane of different compositions with gel. Each series represents an internal volume fraction as displayed in the legend. Horizontal axis represents particle concentration in wt. %.

a) Immediately after deposition of water droplets on the surface. b) 15 seconds after water droplet deposition on the surface.

The water uptake by the functional domains could be explained by strong water absorption capacity of the gel phase dispersed in the membrane formed via emulsion templating method. However, the fact that certain membranes display this behavior while the rest hold the water droplet on the surface with a steady WCA is intriguing. For the case of 0.1 internal volume fraction, water could not be absorbed at any nanoparticle concentration by the membrane, as for this internal volume content, the gel phase was already saturated and could

not absorb water further. For the case of 0.4 % of nanoparticle concentration, water could not be absorbed by the gel phase at any internal volume fraction condition (Figure 4.30) . This could be explained by the fact that at low nanoparticle concentration condition, the droplet sizes are larger and hence not all of the water in the internal phase could be evaporated during drying step, and hence the membrane cannot absorb the water droplet further. The inability of the domains to absorb water could also be explained by the loss of KCOOH during drying or the loosely packed distribution of functional domains which yield considerable SBS areas which has no functionality. Around the domains which include aqueous KCOOH without gel, cracks and cavities form on the particle shells. Thus, the possibility for the former case is sound, since cracked shells cannot function as a potent encapsulation mechanism. The latter case is an additional determinant of surface behavior and is attributed to be the origin of the different behavior of gel samples. The gel membrane samples which show the absorption behavior also corresponds to the samples which comprise closed packed functional domains in microscope images. (Tables 4.1)

In order to demonstrate further that water absorption behavior occurs due to the gel structure, gels containing 1 and 1.5% wt. agar with 0.5 mg/ml KCOOH were prepared and WCA on the surfaces of the gel were measured. Figure 4.31 shows that water could be absorbed by the gel phases formed with both 1 and 1.5 %wt, and that higher agar concentration in the gel solution medium resulted in lower water absorption capacity of the gel. This is explained by higher porosity achieved with lower agar content, which improved water absorption capacity, and hence resulted in lower WCA for low agar containing sample (Figure 4.31). Furthermore the initial water penetration depended significantly on the concentration of the gel structure. The gel which has less concentrated Agar was more hydrophilic than more concentrated gel. The gel sample that consisted 1.5 % Agar yielded roughly half of its contact angle value, decreasing from 44° to 18°. In this study, all of the emulsion templates

comprising gel were prepared by 1% Agar gel and they behave similar to the sole 1% Agar gel.

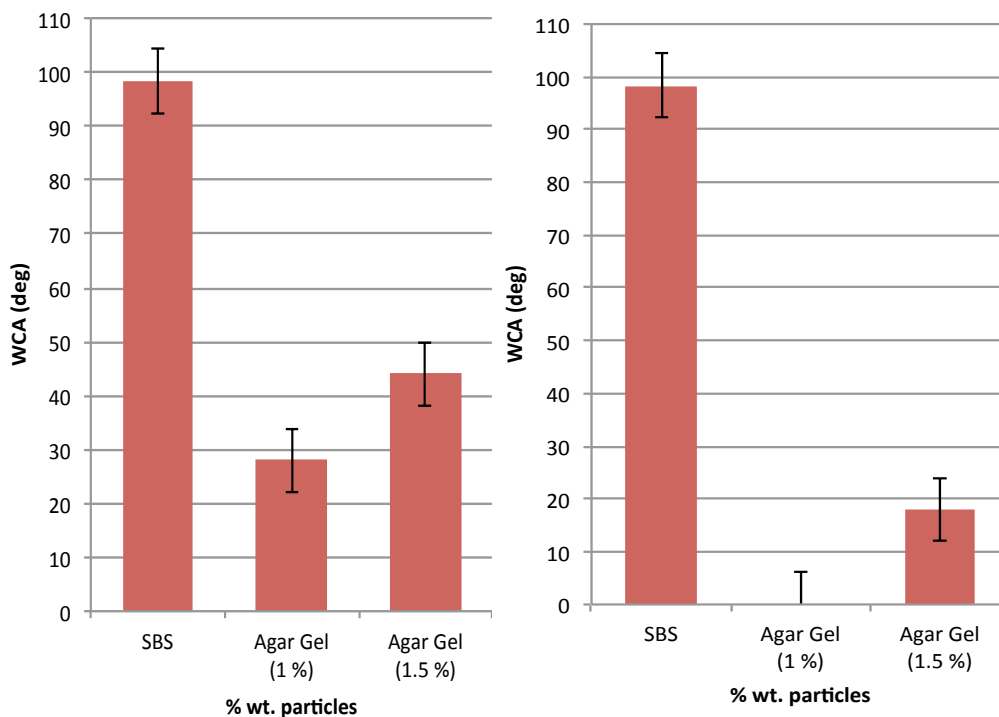


Figure 4.31 WCA ($^{\circ}$) measurements for only SBS coating, 1% wt/vol Agar gel with 0.5 g/ml KCOOH (aq) and 1.5% wt/vol Agar gel with 0.5 g/ml KCOOH (aq) a) Immediately after deposition of water droplets on the surface. b) 15 seconds after water droplet deposition on the surface.

SBS coating on the other hand has no tendency at all for water absorption with its $\sim 97^{\circ}$ WCA staying stable over the time period where water droplet resides on the surface. SBS coating demonstrated a steady, moderately hydrophobic behavior throughout the

observation. It is more hydrophobic than all the membranes which were prepared by templating aqueous phase within SBS phase.

Figure 4.32 displays the samples which showed water absorption behavior and their WCA change over time. It should be noted that all domains displayed in the figure were prepared by 1 % Agar. 1.5 % Agar sample is displayed merely to note the effect of porosity on water absorption capacity.

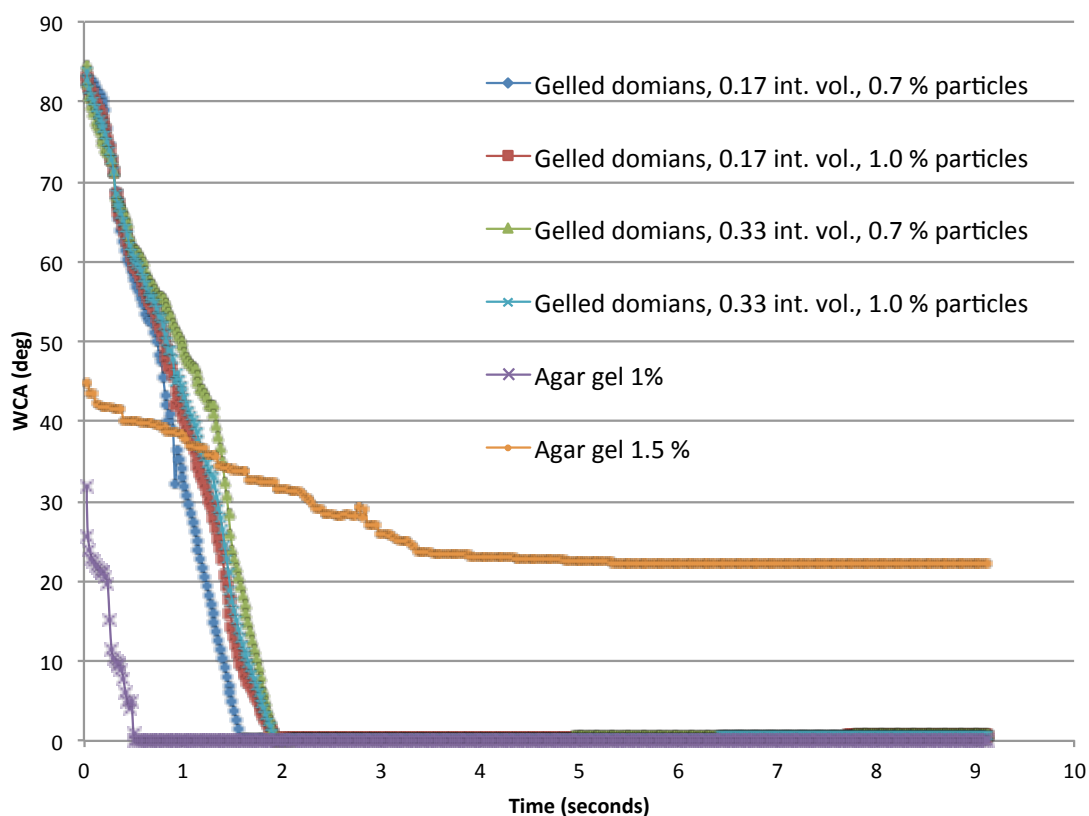


Figure 4.32 Dynamic WCA and its change in time (seconds) for the samples which demonstrate water absorption behavior. All emulsion samples are prepared with 1% Agar gel.

Although the displayed templated membranes containing Agar gel show full water absorption, the absorption rate is much less than that of only Agar gel. This is due to the presence of hydrophobic SBS base that include functional gel domains within the whole membrane structure. The SBS within the membrane retards water absorption. Thus, when the gel domains are unevenly distributed or insufficient in number so that bare SBS membrane is exposed to the water droplet's penetration, water absorption cannot occur. Only the sample membranes on which the salty gel domains cover the surface absorb water. Figure 4.33 shows photographs of the water droplet through the course of being absorbed.



Figure 4.33 5 μ l water droplet on the membrane which was templated from the emulsion of internal volume fraction 0.33, and particle concentration 0.7 % a) immediately after disposal of droplet (WCA = 80°) b) 1.5 seconds after (WCA = 25°) c) 2 seconds after disposal of drop (WCA = 13 °)

Relating Morphological Characteristics to Surface Behavior

Similar to the effect observed with gelation of the internal phase, increasing the particle concentration enhanced stability for all samples. For the samples whose internal phase was gelled, the stability was more emphasized regardless of the internal volume fraction. For the samples that were not gelled, internal volume fraction was shown to have an optimum value

that yielded best stability for each particle concentration. The stability was in correspondence with the droplet size.

Both gelling and the fractional amount of components were determinant of the morphology and the microstructure of the resultant membrane. Two phenomena were premises for the microstructure namely, particle bridging and the surface coverage of droplets. Particle bridging was observed predominantly at low particle concentrations. Limited amount of particles in the system formed monolayers between two droplets and bridged them. This phenomenon is in favor of energy minimization while restricting well distributed functional domains. Full surface coverage is the distribution of functional domains in a way that they remain very well scattered on the SBS membrane surface and do not leave any area with bare SBS polymer. Bridging and surface coverage are closely related. High internal volume fraction yields surface coverage except for the case where particle concentration is too low.

Surface coverage and morphology was determinant factors for the surface behavior in terms of WCA. Whereas the WCA on the samples that were not gelled did not show a particular dependence on the components, membranes that consisted of gel domains were highly dependent on them. As the internal volume fraction increases, surface coverage with aqueous droplets increase, thus WCA falls. When surface is fully covered and the functional domains prohibit any SBS contact to the water droplet the surface, the surface absorb the water droplet completely, dropping the WCA to 0° .

Rheological Characterization

The rheological characterization and comparison of emulsion samples were conducted by oscillatory and flow tests on shear rheometer. For the purpose of maintaining a reliable comparison between rheological behaviors of different emulsions, a sample group whose properties are consistent within each other is sought. Therefore, a sample group which includes exclusively the emulsions which yielded water absorption on dry membrane surfaces has been selected for rheological experiments. Additional to this particular four gelled samples, the non-gel samples with corresponding particle concentration and internal volume fraction are analyzed as well. This selection resulted with a total of 8 samples to be investigated.

The viscosities of the emulsions with respect to shear rate are measured through flow tests. It is apparent that emulsification within SBS solution decreases viscosity as compared to homogeneous SBS dissolved in cyclohexane. (Figure xyz-xyz) SBS solution used for this measurement has the same concentration as the continuous polymer phase of sample emulsions, which is 73 mg/ml. This result is sound since a secondary phase droplets which disturbs continuity in fluid structure weakens. Nanoparticle addition, increasing the internal phase and gelling the internal phase reduces this weakening effect. The only emulsion that flows more viscous than homogeneous SBS solution at all shear rates is the gelled emulsion in which both nanoparticle concentration and the internal volume fraction are maximized (1.0 % and 0.33 respectively). (Figure xyz)

The emulsions with gelled droplets display higher viscosity than the emulsions which had liquid aqueous droplets. As the nanoparticle concentration and the internal volume fraction is increased, the viscosity is increased in both gelled and non-gelled samples. However the enhancing effect of particle concentration and internal phase fraction is more pronounced. The non-gelled sample with less particle concentration and more internal volume fraction

displays an off-balance viscosity dependence on shear rate. (0.7 % and 0.33 respectively) The reason of this fluctuation is attributed to the possibility that 0.7 % of particles do not suffice to stabilize the internal phase under shear. Although the optical microscope images of the wet emulsions of this particular sample do not hint any phase separation or droplet merging, the droplets may fail to sustain their integrity under shear stress applied by the continuous circulation and friction of the rheometer geometry.

The fact that particle addition enhances viscosity is convenient and supported by the literature. Despite that solid particles, like emulsion droplets, disturb the continuity of the fluid morphology, when the non-continuous phase consists particles which are as small as within nano-scale, flow is hindered. The deformation per unit shear stress is reduced. Additionally, increasing particle concentration enhances stability. More stable droplets within emulsion yield higher viscosity. More particles also cause smaller droplets with greater quantity. Increasing the droplet surface area by reducing their size makes way for more interfacial friction among them. The friction increase enhances viscosity. Lastly, the spatial hindrance caused by the increase in droplet number per unit volume causes an increase in viscosity.

Increasing ϕ of both gelled and non-gelled internal phases raises viscosity. This result is intriguing since the maximum viscosity is achieved when no internal phase is added into continuous SBS medium at all, with one exception (0.7 % np concentration and 0.33 ϕ). The fact that the polymer solution is more viscous than aqueous K₂S₂O₈ is orienting to expect non-gelled samples to yield lower viscosity upon higher ϕ . The counter-intuitive increasing dependence of η upon ϕ can be explained by the increase in the total surface area, droplet size reduction and the spatial hindrance caused by the higher amount of internal phase within the emulsion. In an emulsion where the total volume the droplets occupy is higher, the collisions among them increases. The additional friction and collisions which ϕ increase brings along causes an enhancement in viscosity.

All emulsions, consisting both gelled and non-gelled internal droplets show shear thinning behavior. Sole SBS solution on the other hand, shows a linear trend for viscosity upon variance in shear stress. This change in rheological behavior upon emulsification can be attributed to the discontinuity which the droplets create within the undisturbed continuous polymer medium. The shear thinning rate is more in the gelled emulsions relative to the non-gelled ones.

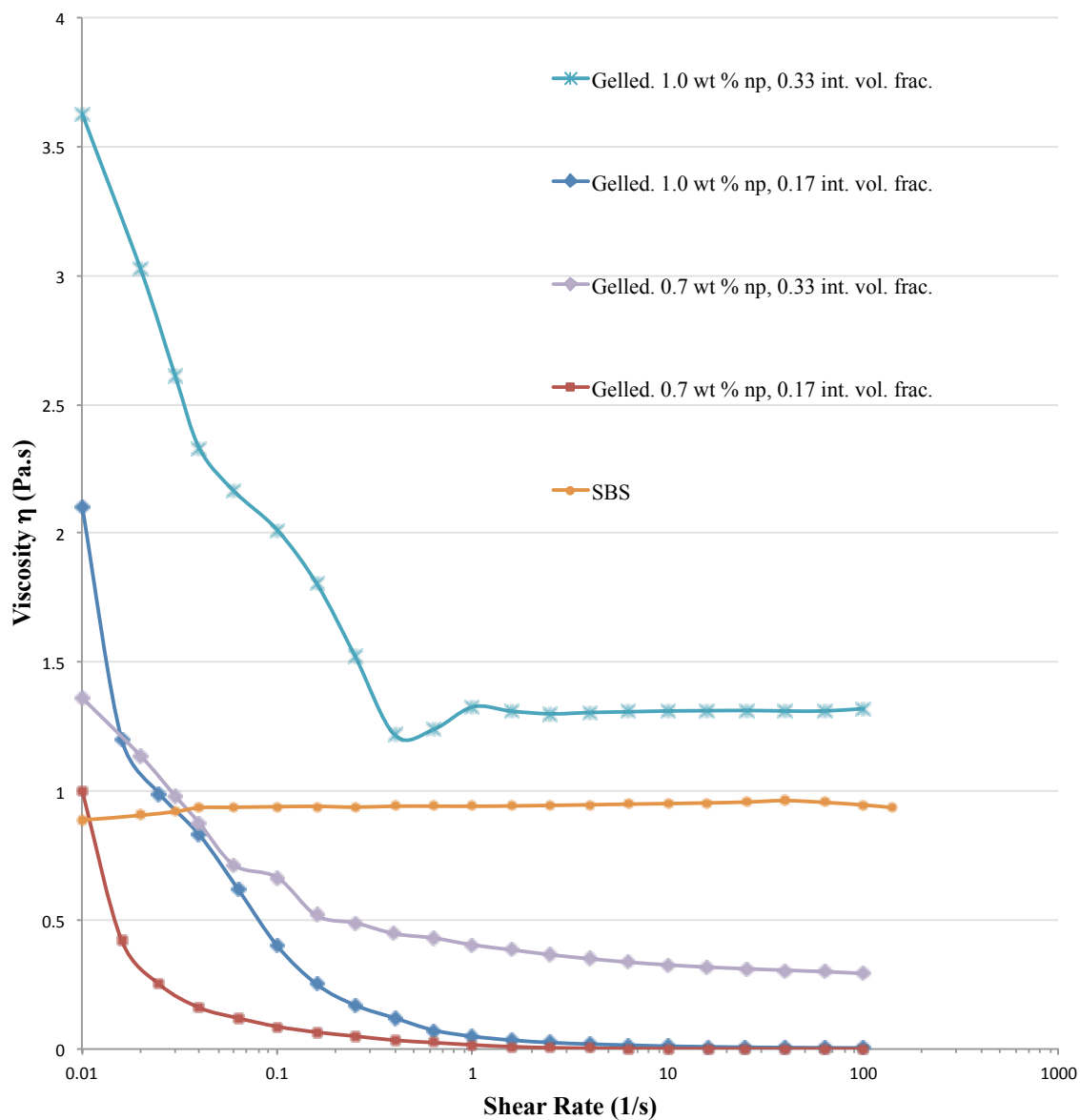


Figure 4.34 Viscosity vs. shear rate plot for four gelled emulsions and homogeneous SBS solution.

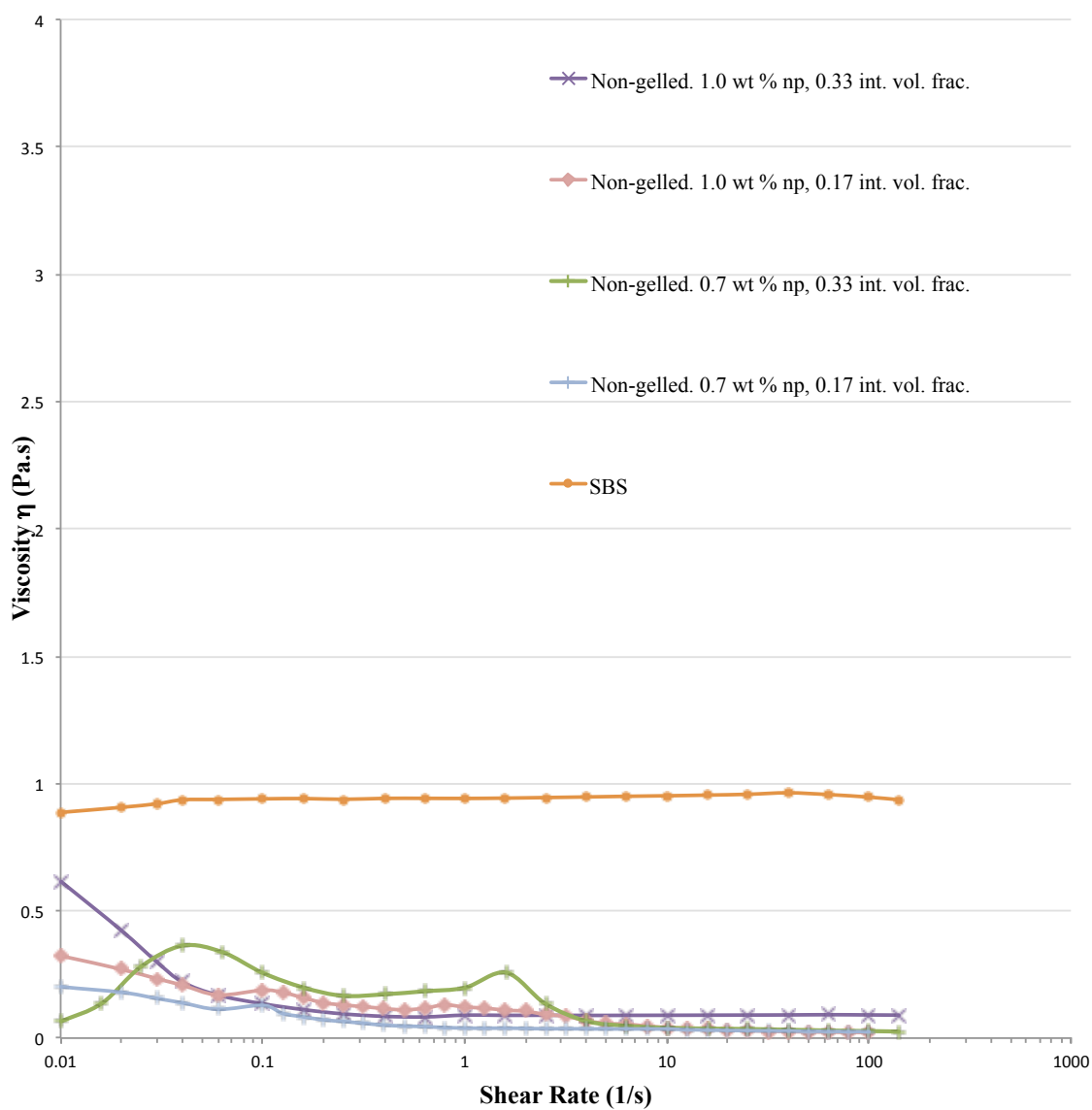


Figure 4.36 Viscosity vs. shear rate plot for four gelled emulsions and homogeneous SBS solution.

G' (storage modulus) and G'' (loss modulus) of a sample pair of gelled and non-gelled emulsions are investigated under oscillatory testing by varying frequency. At low frequencies, the loss modulus is greater than the storage modulus for both gelled and non-gelled emulsions. At a point during frequency increase G' exceeds G'' . The G'' of the gelled sample exceeds G' sooner (at a lower frequency) than of the non-gelled sample. Since G'' is a determinant of the elastic behavior whereas G' indicates viscous behavior, gelating the internal droplets enhances solid-like behavior.

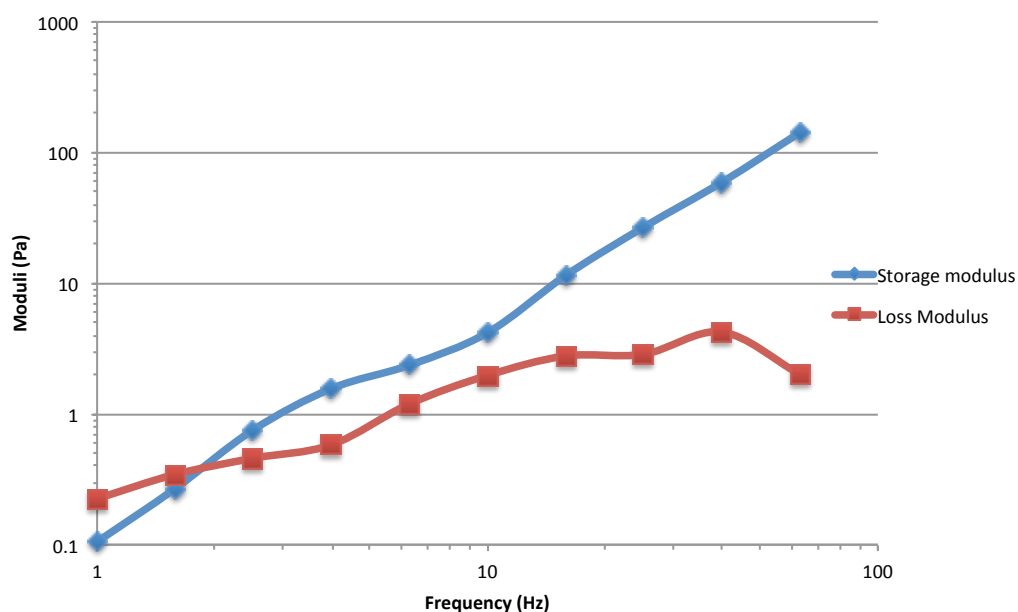


Figure 4.37 Loss and storage moduli in response to frequency for the template emulsion of gel cores, 0.7 % wt. particle concentration and 0.17 internal phase fraction.

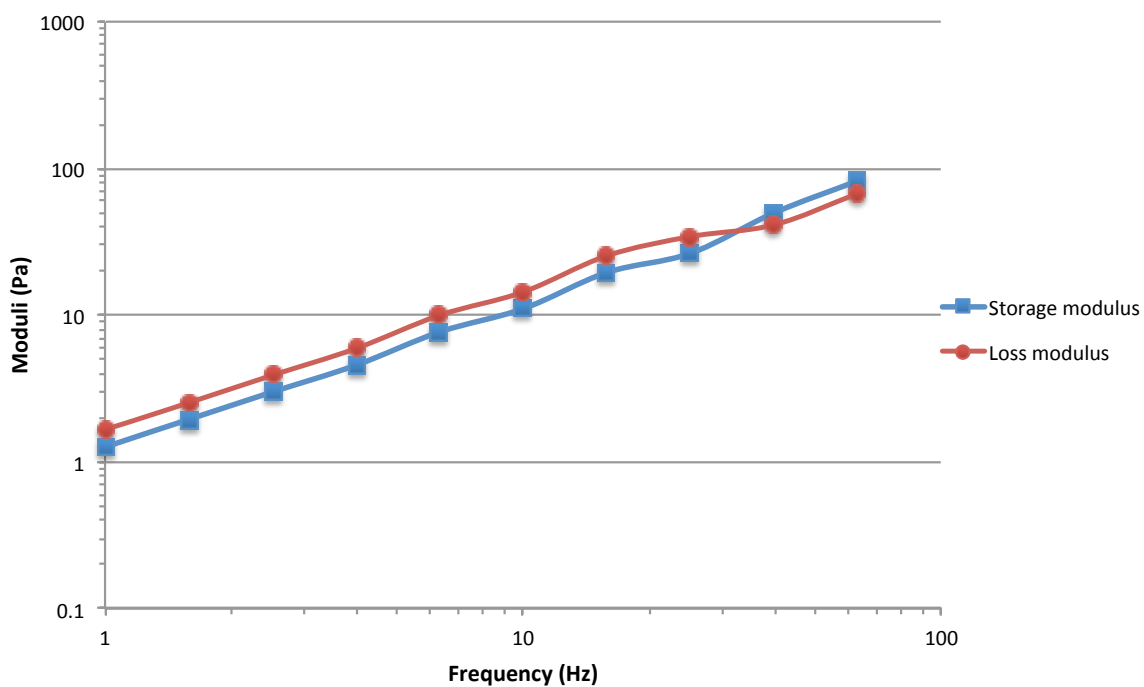


Figure 4.29 Loss and storage moduli in response to frequency for the template emulsion of non-gel cores, 0.7 % wt. particle concentration and 0.17 internal phase fraction.

Chapter 5

CONCLUSION

This study has integrated two well established approaches of emulsion templating in order to produce a hydrophobic membrane which can store hydrophilic materials and release them in a controlled fashion. The first of these approaches utilizes stable emulsions and removes the dispersed hydrophilic droplet phase after gelation or polymerization of the continuous phase. This approach produces porous monoliths where porous structures would form after removal of the droplets. In the second approach, internal droplets are surrounded by a shell of solid particles or a cross linked polymer, which maintains functional individual capsules by purging the continuous phase. Here, neither the continuous nor the dispersed phase is removed. Instead, they were strongly stabilized to compose aqueous delivery capsules embedded in a hydrophobic polymer monolith membrane. The droplets were functionalized by loading with aqueous KCOOH as a representative anti-icing agent. The emulsion was stabilized by solid particle stabilization method, utilizing surface modified partially hydrophobic silica nanoparticles.

The functionalized packages with gel domains were fabricated and compared to the ones without gel domains. The effect of parameters such as gelation, nanoparticle concentration and dispersed phase volume fraction on the stability of the initial emulsion, the rheology of the partially dried viscous emulsion, and on the hydrophobicity and morphology of the

resultant membrane were investigated in detail. Hydrophobicity, water absorption behavior were monitored through gelation of the internal phase droplets, where internal phase volume fraction and particle concentration were changed. The wet emulsions truly serve as templates for the resultant dry membranes since dry forms mimic the wet emulsion in terms of both morphology and water affinity.

There are several advantages of SBS polymer in the continuous medium or the emulsion template. Foremost, SBS shows strong adhesive behavior that can lock the emulsion structure without the need of crosslinking. Additionally, it is possible to crosslink this polymer by UV exposure if necessary. [74] This can prolong to synthesis of three dimensional robust structures in which functional domains of another phase can be incorporated. SBS polymer is widely used to modify bitumen in asphalt construction. Bitumen properties can be improved using an additive polymer (SBS) or by chemically modification. [65, 74-76] SBS viscoelasticity and temperature susceptibility makes it a good candidate to be used in polymer modified bitumen (PMB). [26] Thus, use of SBS in the polymeric composite designed in this study opens the possibility to incorporate anti-icing agent into heterogeneous bitumen used in roadways.

Different from previous studies on emulsion templating, which either obtained a porous monolith or isolated capsules, in this study, functional domains with or without gel phase embedded on a monolith membrane has been prepared, and characterized. The domains can serve as functional capsules which store anti-icing agents and are surrounded by Pickering. To our knowledge, few studies where both continuous and dispersed phases are polymerized to form a membrane have been proposed solely for filtration and have used common surfactants. [34] Thus, utilizing solid particle stabilized droplets, gelation of the functional phase and loading anti-icing agents within the membrane impart novelty to potential applications for similar research areas.

Apart from being utilized as surface coating membrane, the designed functionally loaded material is promising to find future applications such as monolith scaffolds in tissue engineering, platforms for drug delivery from a surface, tool for food processing or coating for delivery of functional anti-icing materials. This encapsulation method is not only applicable to store aqueous KCOOH but it can be extended to any water soluble material.

Since a variety of materials including optically and chemically active materials can be incorporated into macroporous materials [7], the membrane designed here can lead to applications where functional materials other than ionic salts are incorporated into hydrophobic monoliths. Finally, the template emulsion can be designed to serve both as a dry membrane and a viscous stable multiphase system to be integrated into other hydrophobic mediums that would otherwise be incompatible with the delivery material. In order to manipulate the affinity towards various other mediums, other polymers hydrophobic polymers than SBS can be favored. Future work will include rheological characterization of dry material, investigation of the rate of material delivery through the embedded capsules and possible manipulations over it and incorporation of the viscous emulsion to other hydrophobic mediums.

BIBLIOGRAPHY

1. Akartuna, I., et al., *General route for the assembly of functional inorganic capsules*. Langmuir, 2009. **25**(21): p. 12419-24.
2. Akartuna, I., et al., *Macroporous polymers from particle stabilized emulsions*. Polymer, 2009. **50**: p. 3646-3651.
3. Binks, B.P., *Macroporous silica from solid-stabilized emulsion templates*. Advanced Materials, 2002. **14**(24): p. 1824-1827.
4. Cayre, O.J., P.F. Noble, and V.N. Paunov, *Fabrication of novel colloidosome microcapsules with gelled aqueous cores*. Journal of Materials Chemistry, 2004. **14**(22): p. 3351-3355.
5. Haibach, K., et al., *Tailoring mechanical properties of highly porous polymer foams: Silica particle reinforced polymer foams via emulsion templating*. Polymer, 2006. **47**(13): p. 4513-4519.
6. Imhof, A. and D.J. Pine, *Ordered macroporous materials by emulsion templating*. Nature, 1997. **389**(6654): p. 948-951.
7. Imhof, A. and D.J. Pine, *Uniform macroporous ceramics and plastics by emulsion templating*. Chemical Engineering & Technology, 1998. **21**(8): p. 682-685.
8. Menner, A., et al., *Tough reinforced open porous polymer foams via concentrated emulsion templating*. Polymer, 2006. **47**(22): p. 7628-7635.
9. Pulko, I. and P. Krajnc, *Open cellular reactive porous membranes from high internal phase emulsions*. Chem Commun (Camb), 2008(37): p. 4481-3.
10. Wei, Z.X. and M.X. Wan, *Hollow microspheres of polyaniline synthesized with an aniline emulsion template*. Advanced Materials, 2002. **14**(18): p. 1314-+.

11. Zoldesi, C.I. and A. Imhof, *Synthesis of monodisperse colloidal spheres, capsules, and microballoons by emulsion templating*. *Advanced Materials*, 2005. **17**(7): p. 924-+.
12. Aranberri, I., et al., *Synthesis of macroporous silica from solid-stabilised emulsion templates*. *Journal of Porous Materials*, 2009. **16**(4): p. 429-437.
13. Ikem, V.O., et al., *Highly permeable macroporous polymers synthesized from pickering medium and high internal phase emulsion templates*. *Advanced Materials*, 2010. **22**(32): p. 3588-92.
14. Hellsten, P.P., et al., *Use of potassium formate in road winter deicing can reduce groundwater deterioration*. *Environ Sci Technol*, 2005. **39**(13): p. 5095-5100.
15. Hall, D.L., S.M. Sterner, and R.J. Bodnar, *Freezing point depression of NaCl KCl H₂O solutions*. *Economic Geology*, 1988. **83**: p. 197-202.
16. Binks, B.P., *Particles as surfactants - similarities and differences*. *Current Opinion in Colloid & Interface Science*, 2002. **7**(1-2): p. 21-41.
17. Melle, S., M. Lask, and G. Fuller, *Pickering emulsions with controllable stability*. *Langmuir*, 2004. **21**: p. 2158-2162.
18. Pickering, S.U., *Emulsions*. *J. Chem. Soc.*, 1907. **91**(2001).
19. Ramsden, W., *Separation of Solids in the Surface-Layers of Solutions and 'Suspensions' (Observations on Surface-Membranes, Bubbles, Emulsions, and Mechanical Coagulation)*. *Proc. R. Soc.*, 1903. **72**(156).
20. Airey, G.D., *Rheological properties of styrene butadiene styrene polymer modified road bitumens*. *Fuel*, 2003. **82**.
21. Hanyu, A., et al., *Effect of the morphology of SBS modified asphalt on mechanical properties of binder and mixture* *Journal of the Eastern Asia Society for Transportation Studies*, 2005. **6**.

22. Lesueur, D., *The colloidal structure of bitumen: Consequences on the rheology and on the mechanisms of bitumen modification*. Advances in Colloid and Interface Science, 2009. **145**: p. 42–82.
23. Liu, Z., et al., *A Study of the Compatibility Between Asphalt and SBS*. Petroleum Science and Technology, 2003. **21**: p. 1317-1325.
24. Lu, X. and U. Isacsson, *Influence of styrene-butadiene- styrene polymer modification on bitumen viscosity*. Fuel, 1997. **76**: p. 1353-1359.
25. Lu, X. and U. Isacsson, *Chemical and rheological evaluation of ageing properties of SBS polymer modified bitumens*. Fuel, 1998. **77**: p. 961-972.
26. Lu, X., U. Isacsson, and J. Ekblad, *Phase separation of SBS polymer modified bitumens*. Journal of Materials in Civil Engineering, 1999. **11**: p. 51-57.
27. Perez-Lepe, A., et al., *Influence of the processing conditions on the rheological behaviour of polymer-modified bitumen*. Fuel, 2003. **82**: p. 1339-1348.
28. Sengoz, B. and G. Isikyakar, *Analysis of styrene-butadiene-styrene polymer modified bitumen using fluorescent microscopy and conventional test methods*. Journal of Hazardous Materials, 2008. **150**.
29. Topal, A., et al., *Evaluation of Rheological and Image Properties of Styrene-Butadiene-Styrene and Ethylene-Vinyl Acetate Polymer Modified Bitumens*. Journal of Applied Polymer Science, 2011. **122**: p. 3122-3132.
30. Yildirim, Y., *Polymer modified asphalt binders*. Construction and Building Materials 2007. **21**: p. 66-72.
31. Busby, W., N.R. Cameron, and A.B.C. Jahoda, *Tissue engineering matrixes by emulsion templating*. Polymer International, 2002. **51**(10): p. 871-881.
32. Dubois, R. and P.Y. Dubois, *Process for preventing formation of black ice on roads by applying a mixture of salt and aqueous fixation composition onto the road surface*, 1984, Selfixat, S. A.: Switzerland.

33. Pulko, I., et al., *Ultra-high surface area functional porous polymers by emulsion templating and hypercrosslinking: efficient nucleophilic catalyst supports*. Chemistry, 2010. **16**(8): p. 2350-4.
34. Ruckenstein, E. and C.H. H., *Preparation of a water - permselective composite membrane by the concentrated emulsion method: Its swelling and permselectivity characteristics*. Journal of Applied Polymer Science, 1991. **42**(9): p. 2429–2434.
35. Duan, H., et al., *Magnetic colloidosomes derived from nanoparticle interfacial self-assembly*. Nano Lett, 2005. **5**(5): p. 949-52.
36. Rothstein, J.P., *Slip on Superhydrophobic Surfaces*. Annual Review of Fluid Mechanics, 2010. **42**: p. 89-109.
37. Kulinich, S.A., et al., *Superhydrophobic surfaces: are they really ice-repellent?* Langmuir, 2011. **27**(1): p. 25-9.
38. He, M., et al., *Super-hydrophobic surfaces to condensed micro-droplets at temperatures below the freezing point retard ice/frost formation*. Soft Matter, 2010. **7**: p. 3993-4000.
39. He, M., et al., *Super-hydrophobic film retard frost formation*. Soft Matter, 2010. **6**: p. 2396-2399.
40. Feuillebois, F., M.Z. Bazant, and O.I. Vinogradova, *Effective slip over superhydrophobic surfaces in thin channels*. Phys Rev Lett, 2009. **102**(2): p. 026001.
41. Alizadeh, A., et al., *Dynamics of Ice Nucleation on Water Repellent Surfaces*. Langmuir, 2012. **28**: p. 3180-3186.
42. Bahadur, V., et al., *Predictive Model for Ice Formation on Superhydrophobic Surfaces*. Langmuir, 2011. **27**: p. 14143-14150.
43. Dubois, R., *De-icing compositions contained in road surface material*, in *Washington Post*, L. La Croix, Editor 1977, Plastiroute SA.

44. Lee, M.N., H.K. Chan, and A. Mohraz, *Characteristics of pickering emulsion gels formed by droplet bridging*. Langmuir, 2012. **28**(6): p. 3085-91.
45. Dai, L.L., *Self-assembled structure of nanoparticles at a liquid-liquid interface*. Langmuir, 2005. **21**: p. 2641-2643.
46. Lin, Y., et al., *Nanoparticle assembly at fluid interfaces: structure and dynamics*. Langmuir, 2005. **21**: p. 191-194.
47. Pickering, E.C., *Photographs of Faint Stars*. Science, 1907. **25**(637): p. 435-7.
48. Lin, Y., et al., *Nanoparticle assembly and transport at liquid-liquid interfaces*. Science, 2003. **299**(5604): p. 226-9.
49. Niu, Z., et al., *Synthesis of nano/microstructures at fluid interfaces*. Angew Chem Int Ed Engl, 2010. **49**(52): p. 10052-66.
50. Ikem, V.O., A. Menner, and A. Bismarck, *High Internal Phase Emulsions Stabilized Solely by Functionalized Silica Particles*. Angewandte Chemie-International Edition, 2008. **47**(43): p. 8277-8279.
51. Velikov, K.P. and O.D. Velev, *Stabilization of thin films, foams, emulsions and bifluid gels with surface-active solid particles*, in *Colloid Stability and Application in Pharmacy*, T.F. Tadros, Editor 2007, WILEY-VCH: Weinheim. p. 277-306.
52. Velikov, K.P. and O.D. Velev, *Stabilization of thin films, foams, emulsions, and biliquid gels with surface active solid particles*. Colloid stability and application in pharmacy, ed. T.F. Tadros. Vol. 3. 2007, Weinheim: Wiley vch.
53. Binks, B.P., *Particles as surfactants—similarities and differences*. Current Opinion in Colloid & Interface Science, 2002. **7**(1-2): p. 21-41.
54. Paunov, V.N., *Novel method for determining the three-phase contact angle of colloid particles adsorbed at air-water and oil-water interfaces*. Langmuir, 2003. **19**: p. 7970-7976.

55. Stejskal, J., et al., *Polyaniline dispersions .6. Stabilization by colloidal silica particles*. *Macromolecules*, 1996. **29**(21): p. 6814-6819.
56. Noble, P.F., et al., *Fabrication of "hairy" colloidosomes with shells of polymeric microrods*. *J Am Chem Soc*, 2004. **126**(26): p. 8092-8093.
57. Ashby, N.P., B.P. Binks, and V.N. Paunov, *Bridging interaction between a water drop stabilised by solid particles and a planar oil/water interface*. *Chem Commun (Camb)*, 2004(4): p. 436-7.
58. Frost, D.S., et al., *Understanding droplet bridging in ionic liquid-based Pickering emulsions*. *J Colloid Interface Sci*, 2012. **383**(1): p. 103-9.
59. Horozov, T.S., et al., *Particle zips: vertical emulsion films with particle monolayers at their surfaces*. *Langmuir*, 2005. **21**(6): p. 2330-41.
60. Thieme, J., S. Abend, and G. Lagaly, *Aggregation in pickering emulsions*. *Colloid Polym Sci*, 1999. **277**: p. 257-260.
61. Tambe, D. and A. Sharma, *Adv. Colloid Interface Sci.*, 1994. **52**.
62. Nakagawa, N. and Y. Nonomura, *Drying process of emulsions stabilized by solid particles*. *Chem. Lett.*, 2011. **40**: p. 818-819.
63. Wang, C., et al., *Facile fabrication of hybrid colloidosomes with alginate gel cores and shells of porous CaCO₃ microparticles*. *Chemphyschem*, 2007. **8**(8): p. 1157-60.
64. Dinsmore, A.D., et al., *Colloidosomes: Selectively permeable capsules composed of colloidal particles*. *Science*, 2002. **298**(5595): p. 1006-1009.
65. You, Z., et al., *Nanoclay-modified asphalt materials: Preparation and characterization* *Construction and Building Materials*, 2011: p. 1072-1078.
66. Matheson, R.R., Jr., *20th- to 21st-century technological challenges in soft coatings*. *Science*, 2002. **297**(5583): p. 976-9.

67. Madej, W., et al., *Breath figures in polymer and polymer blend films spin-coated in dry and humid ambience*. Langmuir, 2008. **24**(7): p. 3517-24.
68. Boker, A., et al., *Hierarchical nanoparticle assemblies formed by decorating breath figures*. Nat Mater, 2004. **3**(5): p. 302-6.
69. Robidoux, P.Y. and C.E. Delisle, *Ecotoxicological evaluation of three deicers (NaCl, NaFo, CMA)-effect on terrestrial organisms*. Ecotoxicol Environ Saf, 2001. **48**(2): p. 128-39.
70. Locke, D.E., et al., *A study of corrosion properties of a new deicer, calcium magnesium acetate*. Transp. Res. Record, 1987. **1113**: p. 30-38.
71. French, H.K., S.E.A.T.M. Van der Zee, and A. Leijnse, *Transport and degradation of propyleneglycol and potassium acetate in the unsaturated zone*. Journal of Contaminant Hydrology, 2001. **49**(1-2): p. 23-48.
72. Simovic, S. and C.A. Prestidge, *Nanoparticles of varying hydrophobicity at the emulsion droplet-water interface: Adsorption and coalescence stability*. Langmuir, 2004. **20**(19): p. 8357-8365.
73. Ding, P., M.G. Orwa, and A.W. Pacek, *De-agglomeration of hydrophobic and hydrophilic silica nano-powders in a high shear mixer*. Powder Technology, 2009. **195**(3): p. 221-226.
74. Staeger, M., et al., *Surface investigation of adhesive formulation consisting of UV sensitive triblock poly(styrene-b-butadiene-b-styrene) copolymer*. Applied Surface Science, 2002. **185**: p. 231-242.
75. Chen, H. and Q. Xu, *Experimental study of fibers in stabilizing and reinforcing asphalt binder*. Fuel, 2010. **89**: p. 1616-1622.
76. Goh, S.W., et al., *Effect of deicing solutions on the tensile strength of micro or nano-modified asphalt mixture*. Construction and Building Materials, 2011. **25**: p. 195-200.

VITA

Selin Kanyas was born in İzmir, Turkey in 1989. She has graduated from American Collegiate Institute in İzmir in 2006. Same year, she started her undergraduate education in Chemical and Biological Engineering Department in Koç University, İstanbul. In 2010 she received her B.S. degree and joined Materials Science and Engineering Department in Koç University as a M.S. student. Her current research interests are polymeric composite materials, nanomaterials and biomimicry.